

Supporting Information

**Probing Long-Range Coupling in Cyclic Silanes**

John T. Ferguson, Qifeng Jiang, Eric A. Marro, Maxime A. Siegler, Rebekka S. Klausen<sup>a,\*</sup>

<sup>a</sup>Department of Chemistry, Johns Hopkins University, 3400 N. Charles St., Baltimore, Maryland 21218, United States.

Corresponding e-mail: klausen@jhu.edu

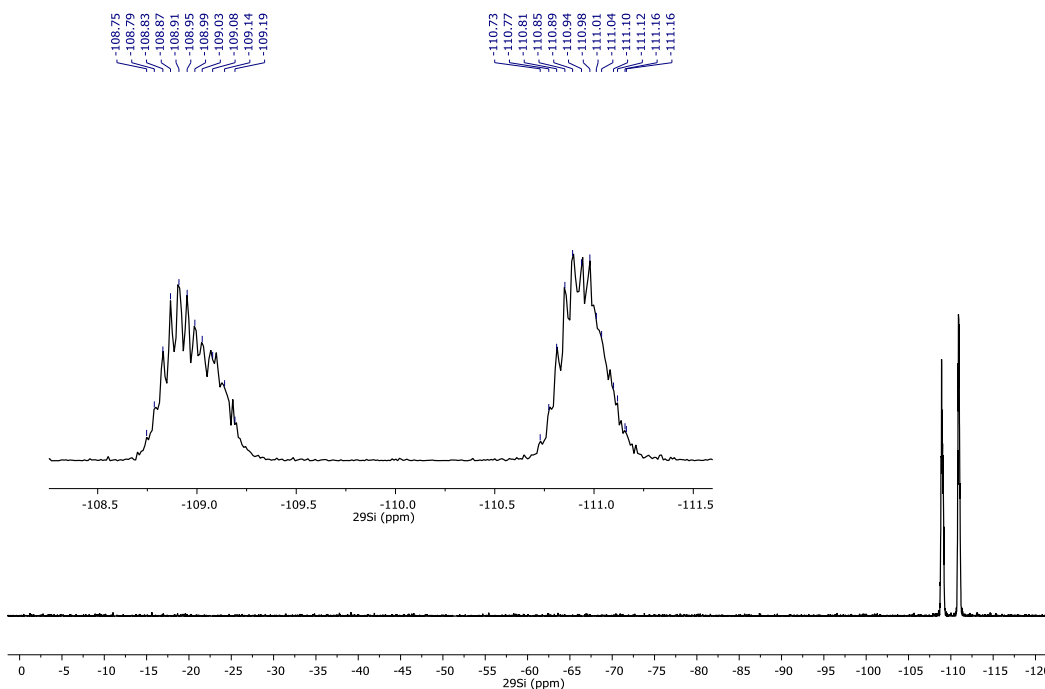
**Table of Contents**

1.	Supplemental Figures and Tables	<b>S-2</b>
2.	NMR Spectra	<b>S-15</b>
3.	Single Crystal X-Ray Crystallography	<b>S-27</b>
4.	References	<b>S-34</b>

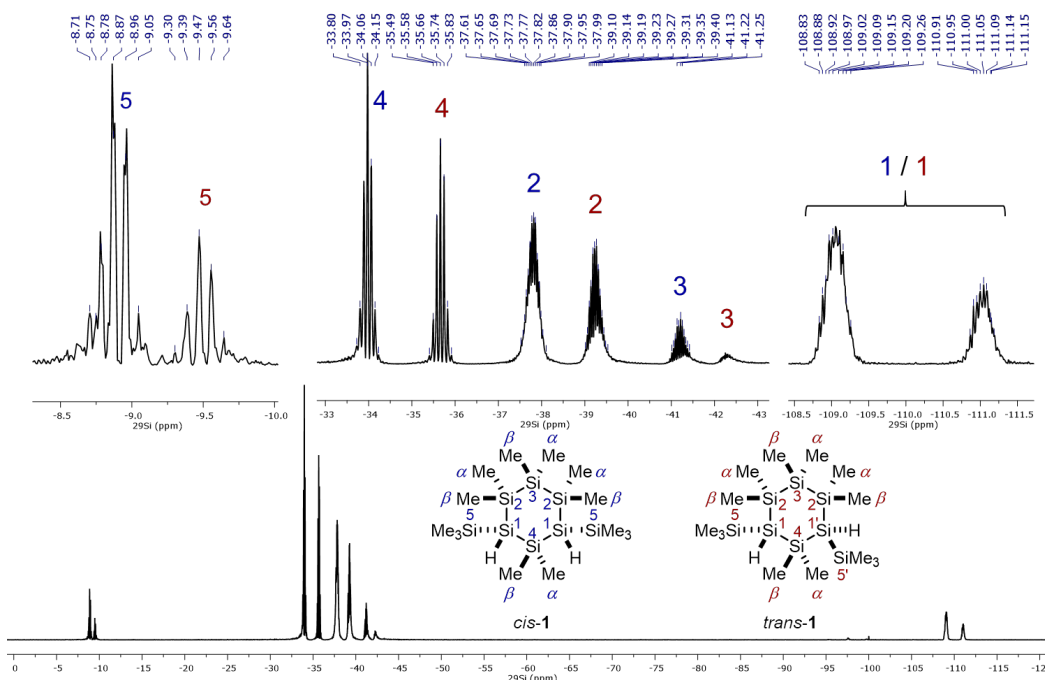
## 1. Supplementary Figures

**Table S-1.** Bond lengths, angles, and dihedral angles in the crystal structure of  $7^{2-} \cdot 2[K(18\text{-cr-6})]^+$

<b>Si – Si Bond</b>	<b>Bond Length (Angstroms)</b>
Si1 – Si2	2.35140
Si2 – Si3	2.33389
Si3 – Si4	2.34634
Si4 – Si5	2.33861
Si5 – Si6	2.32151
Si6 – Si1	2.34830
Si2 – Si7	2.33876
Si6 – Si8	2.33067
<b>Si – Si – Si Angle</b>	<b>Angle (Degrees)</b>
Si1 – Si2 – Si3	101.62740
Si2 – Si3 – Si4	110.25870
Si3 – Si4 – Si5	114.68332
Si4 – Si5 – Si6	110.16820
Si5 – Si6 – Si1	102.17405
Si6 – Si1 – Si2	105.08726
Si1 – Si2 – Si7	106.30995
Si7 – Si2 – Si3	102.07533
Si8 – Si6 – Si1	105.42806
Si5 – Si6 – Si8	100.39959
<b>Si – Si – Si – Si Dihedral Angle</b>	<b>Angle (Degrees)</b>
Si1 – Si2 – Si3 – Si4	-60.39319
Si2 – Si3 – Si4 – Si5	48.37851
Si3 – Si4 – Si5 – Si6	-48.24828
Si4 – Si5 – Si6 – Si1	60.46610
Si5 – Si6 – Si1 – Si2	-78.74291
Si6 – Si1 – Si2 – Si3	78.42035
Si7 – Si2 – Si1 – Si6	-175.15549
Si7 – Si2 – Si3 – Si4	-170.10109
Si8 – Si6 – Si1 – Si2	176.71420
Si8 – Si6 – Si5 – Si4	168.90460

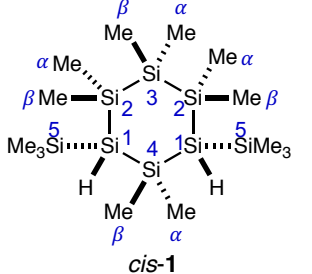
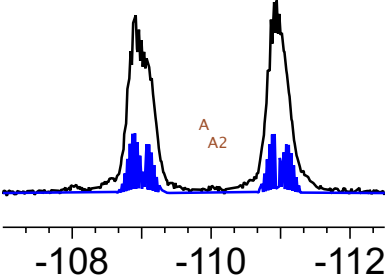
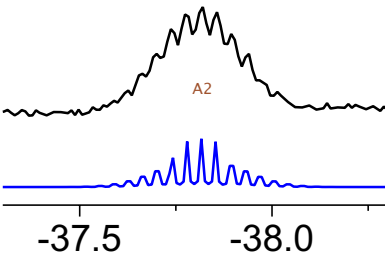


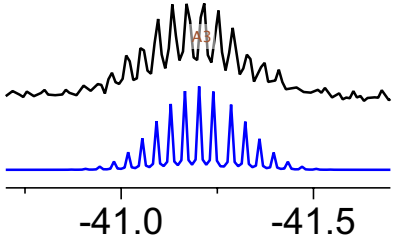
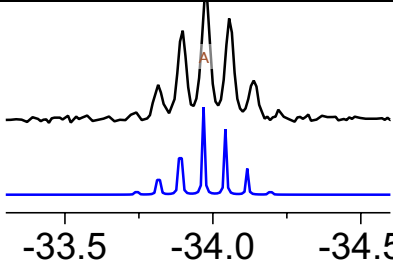
**Figure S1.**  $^{29}\text{Si}$  INEPT+ NMR spectrum (79 MHz,  $\text{C}_6\text{D}_6$ ) of **1** (55:45 *cis:trans*).  $J_X = 160$  Hz to emphasize silicon atoms with one-bond  $^1\text{H}$ - $^{29}\text{Si}$  correlations. Insets show multiplets assigned to both isomers of Si-1 overlapped.

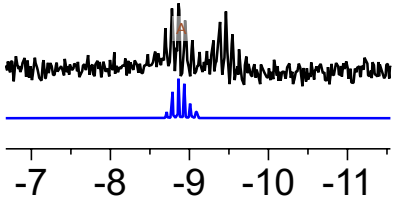
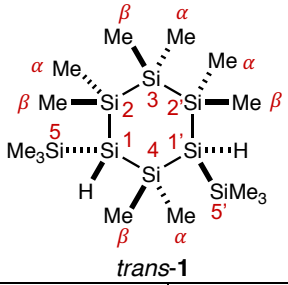
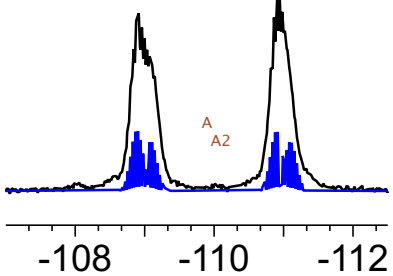


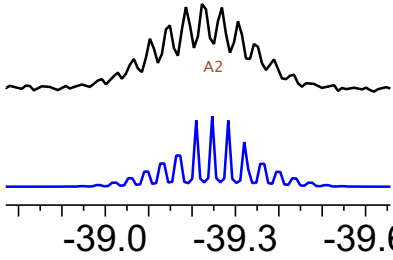
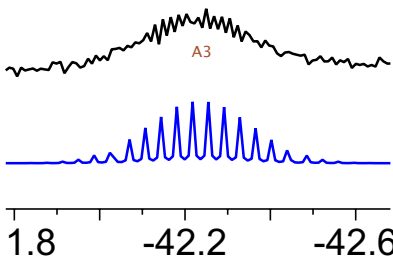
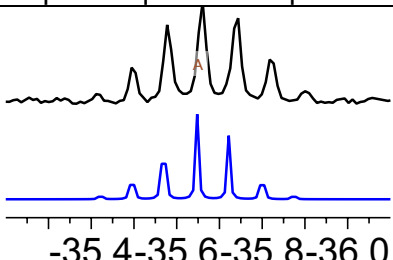
**Figure S2.**  $^{29}\text{Si}$  INEPT+ NMR spectrum (79 MHz,  $\text{C}_6\text{D}_6$ ) of **1** (55:45 *cis:trans*).  $J_X = 7$  Hz to emphasize silicon atoms with two- and three-bond  $^1\text{H}$ - $^{29}\text{Si}$  correlations. Insets show multiplets assigned to Si-4, Si-2, and Si-3. Assignments for *cis*-1 and *trans*-1 indicated in blue and red respectively.

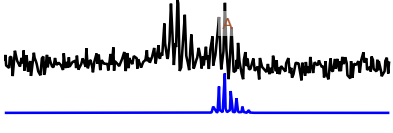
**Table S2. 1** (55:45 *cis:trans*): Multiplet analysis and comparison of experimental and simulated  $^{29}\text{Si}$  INEPT+ spectra. Spin simulation performed in MestReNova 14.1.2.

Cis-1	 <p style="text-align: center;"><i>cis-1</i></p>			Experimental multiplet (black) and superimposed spin simulation (blue)
Silicon #; ppm	$^1\text{J}$ (N)	$^2\text{J}$ (N)	$^3\text{J}$ (N)	
Si-1	<b>A:</b> $^1\text{J}_{\text{Si1-H}}$ (1)	—	<b>B:</b> $^3\text{J}_{\text{Si1-Si5-C-H}}$ (9) <b>C:</b> $^3\text{J}_{\text{Si1-Si2-C-H}\alpha}$ (3) <b>D:</b> $^3\text{J}_{\text{Si1-Si2-C-H}\beta}$ (3) <b>E:</b> $^3\text{J}_{\text{Si1-Si4-C-H}\alpha}$ (3) <b>F:</b> $^3\text{J}_{\text{Si1-Si4-C-H}\beta}$ (3)	 <p style="text-align: center;">-108    -110    -112</p> <p>Experimental spectra: the doublets of multiplets for <i>cis</i>- and <i>trans</i>-1 overlap.  <u>Simulation details, <i>cis</i>-1</u>            (population = 1.22)            A: <math>\delta</math> -109.9 (N = 1, spin = <math>\frac{1}{2}</math>)            B: <math>\delta</math> 250 (N = 1, spin = <math>\frac{1}{2}</math>)            C: <math>\delta</math> 251 (N = 21, spin = <math>\frac{1}{2}</math>)  <math>J_{\text{A-B}} = 160</math> Hz  <math>J_{\text{A-C}} = 3</math> Hz  <u>Simulation details, <i>trans</i>-1</u>            (population = 1.00)            A2: <math>\delta</math> -110.1 (N = 1, spin = <math>\frac{1}{2}</math>)            B2: <math>\delta</math> 250 (N = 1, spin = <math>\frac{1}{2}</math>)            C2: <math>\delta</math> 251 (N = 21, spin = <math>\frac{1}{2}</math>)  <math>J_{\text{A-B}} = 160</math> Hz  <math>J_{\text{A-C}} = 3</math> Hz</p>
Si-2	—	<b>A:</b> $^2\text{J}_{\text{Si2-Si1-H}}$ (1) <b>B:</b> $^2\text{J}_{\text{Si2-C-H}\alpha}$ (3) <b>C:</b> $^2\text{J}_{\text{Si2-C-H}\beta}$ (3)	<b>D:</b> $^3\text{J}_{\text{Si2-Si3-C-H}\alpha}$ (3) <b>E:</b> $^3\text{J}_{\text{Si2-Si3-C-H}\beta}$ (3)	 <p style="text-align: center;">-37.5    -38.0</p> <p>Apparent doublet of doublets of pentets (<math>J = 9.4, 6.0, 3.1</math> Hz)</p>

				<p><b>Simulation details</b>  A: <math>\delta</math> -37.82 (N = 1, spin = <math>\frac{1}{2}</math>)  B: <math>\delta</math> 2 (N = 1, spin = <math>\frac{1}{2}</math>)  C: <math>\delta</math> 3 (N = 3, spin = <math>\frac{1}{2}</math>)  D: <math>\delta</math> 4 (N = 3, spin = <math>\frac{1}{2}</math>)  E: <math>\delta</math> 5 (N = 3, spin = <math>\frac{1}{2}</math>)  F: <math>\delta</math> 6 (N = 3, spin = <math>\frac{1}{2}</math>)  <math>J_{A-B}</math> = 0.5 Hz  <math>J_{A-C}</math> = 6 Hz  <math>J_{A-D}</math> = 6 Hz  <math>J_{A-E}</math> = 3 Hz  <math>J_{A-F}</math> = 3 Hz  quartet of quartets of doublets</p>
Si-3	—	<p><b>A:</b> <math>{}^2J_{Si3-C-H\beta}</math> (3)  <b>B:</b> <math>{}^2J_{Si3-C-H\alpha}</math> (3)</p>	<p><b>C:</b> <math>{}^3J_{Si2-Si3-C-H\alpha}</math> (3)  <b>D:</b> <math>{}^3J_{Si2-Si3-C-H\beta}</math> (3)</p>	 <p>Apparent doublet of doublets of quartets (J = 9.0, 6.1, 3.0 Hz)  <b>Simulation details</b>  A: <math>\delta</math> -41.21 (N = 1, spin = <math>\frac{1}{2}</math>)  B: <math>\delta</math> 2 (N = 3, spin = <math>\frac{1}{2}</math>)  C: <math>\delta</math> 3 (N = 3, spin = <math>\frac{1}{2}</math>)  D: <math>\delta</math> 4 (N = 3, spin = <math>\frac{1}{2}</math>)  E: <math>\delta</math> 5 (N = 3, spin = <math>\frac{1}{2}</math>)  <math>J_{A-B}</math> = 6 Hz  <math>J_{A-C}</math> = 6 Hz  <math>J_{A-D}</math> = 3 Hz  <math>J_{A-E}</math> = 3 Hz  quartet of quartets of quartets of quartets</p>
Si-4	—	<p><b>A:</b> <math>{}^2J_{Si4-Si1-H}</math> (1)  <b>B:</b> <math>{}^2J_{Si4-C-H\alpha}</math> (3)  <b>C:</b> <math>{}^2J_{Si4-C-H\beta}</math> (3)</p>	—	 <p>Apparent heptet (J = 6.6 Hz)  <b>Simulation details</b>  A: <math>\delta</math> -33.97  B: <math>\delta</math> 2  C: <math>\delta</math> 3  D: <math>\delta</math> 4  <math>J_{A-B}</math> = 0.4 Hz (1)  <math>J_{A-C}</math> = 6 Hz (3)</p>

				$J_{A-D} = 6 \text{ Hz (3)}$ quartet of quartets of doublets
Si-5	—	<b>A:</b> $^2J_{\text{Si5-Si1-H}} (1)$ <b>B:</b> $^2J_{\text{Si5-C-H}} (9)$	—	 <p>Simulation details</p> <p>A: <math>\delta -8.9</math> (N = 1, spin = <math>\frac{1}{2}</math>)            B: <math>\delta 250</math> (N = 1, spin = <math>\frac{1}{2}</math>)            C: <math>\delta 251</math> (N = 9, spin = <math>\frac{1}{2}</math>)  <math>J_{A-B} = 0.4 \text{ Hz}</math>  <math>J_{A-C} = 6 \text{ Hz}</math>            Decet of doublets</p>
Trans-1	 <p style="text-align: center;"><i>trans-1</i></p>			
Si-1	<b>A:</b> $^1J_{\text{Si1-H}} (1)$	—	<b>B:</b> $^3J_{\text{Si1-Si5-C-H}} (9)$ <b>C:</b> $^3J_{\text{Si1-Si2-C-H}\alpha} (3)$ <b>D:</b> $^3J_{\text{Si1-Si2-C-H}\beta} (3)$ <b>E:</b> $^3J_{\text{Si1-Si4-C-H}} (6)$	 <p>Experimental spectra: the doublets of multiplets for cis- and trans-1 overlap.</p> <p>Simulation details, cis-1 (weighted 1.22)</p> <p>A: <math>\delta -109.9</math> (N = 1, spin = <math>\frac{1}{2}</math>)            B: <math>\delta 250</math> (N = 1, spin = <math>\frac{1}{2}</math>)            C: <math>\delta 251</math> (N = 21, spin = <math>\frac{1}{2}</math>)  <math>J_{A-B} = 160 \text{ Hz}</math>  <math>J_{A-C} = 3 \text{ Hz}</math></p> <p>Simulation details, trans-1 (weighted 1.00)</p> <p>A2: <math>\delta -110.1</math> (N = 1, spin = <math>\frac{1}{2}</math>)            B2: <math>\delta 250</math> (N = 1, spin = <math>\frac{1}{2}</math>)            C2: <math>\delta 251</math> (N = 21, spin = <math>\frac{1}{2}</math>)  <math>J_{A-B} = 160 \text{ Hz}</math></p>

Si-2, Si-2'	—	<b>A:</b> $^2J_{\text{Si}2\text{-C-H}\alpha}$ (3) <b>B:</b> $^2J_{\text{Si}2\text{-C-H}\beta}$ (3) <b>C:</b> $^2J_{\text{Si}2\text{-Si}1\text{-H}}$ (1)	<b>D:</b> $^3J_{\text{Si}2\text{-Si}3\text{-C-H}}$ (6)	$J_{\text{A-C}} = 3 \text{ Hz}$  <p>Apparent doublet of doublets of heptets (<math>J = 10.0, 7.0, 3.0</math>)  <u>Simulation details</u>  A: <math>\delta -39.25</math> (<math>N = 1</math>, spin = <math>\frac{1}{2}</math>)  B: <math>\delta 2</math> (<math>N = 1</math>, spin = <math>\frac{1}{2}</math>)  C: <math>\delta 3</math> (<math>N = 3</math>, spin = <math>\frac{1}{2}</math>)  D: <math>\delta 4</math> (<math>N = 3</math>, spin = <math>\frac{1}{2}</math>)  E: <math>\delta 5</math> (<math>N = 6</math>, spin = <math>\frac{1}{2}</math>)  <math>J_{\text{A-B}} = 0.5 \text{ Hz}</math>  <math>J_{\text{A-C}} = 6 \text{ Hz}</math>  <math>J_{\text{A-D}} = 6 \text{ Hz}</math>  <math>J_{\text{A-E}} = 3 \text{ Hz}</math>  Quartet of quartets of heptets of doublets </p>
Si-3	—	<b>A:</b> $^2J_{\text{Si}3\text{-C-H}}$ (6)	<b>B:</b> $^3J_{\text{Si}3\text{-Si}2\text{-C-H}\alpha}$ (3) <b>C:</b> $^3J_{\text{Si}3\text{-Si}2\text{-C-H}\beta}$ (3)	 <p>Apparent broad singlet  Simulation  <u>Simulation details</u>  A: <math>\delta -42.24</math> (<math>N = 1</math>, spin = <math>\frac{1}{2}</math>)  B: <math>\delta 2</math> (<math>N = 6</math>, spin = <math>\frac{1}{2}</math>)  C: <math>\delta 3</math> (<math>N = 3</math>, spin = <math>\frac{1}{2}</math>)  D: <math>\delta 4</math> (<math>N = 3</math>, spin = <math>\frac{1}{2}</math>)  <math>J_{\text{A-B}} = 6 \text{ Hz}</math>  <math>J_{\text{A-C}} = 6 \text{ Hz}</math>  <math>J_{\text{A-E}} = 3 \text{ Hz}</math>  Heptet of quartets of quartets </p>
Si-4	—	<b>A:</b> $^2J_{\text{Si}4\text{-Si}1\text{-H}}$ (1) <b>B:</b> $^2J_{\text{Si}4\text{-C-H}}$ (6)	—	 <p>Apparent heptet (<math>J = 6.5 \text{ Hz}</math>)</p>

				<p><b>Simulation details</b>  A: <math>\delta</math> -35.6 (N = 1, spin = <math>\frac{1}{2}</math>)  B: <math>\delta</math> 2 (N = 1, spin = <math>\frac{1}{2}</math>)  C: <math>\delta</math> 3 (N = 6, spin = <math>\frac{1}{2}</math>)  <math>J_{A-B}</math> = 0.5 Hz  <math>J_{A-C}</math> = 6 Hz  Heptet of doublets</p>
Si-5, Si-5'	—	<p><b>A:</b> <math>{}^2J_{Si5-Si1-H}</math> (1)  <b>B:</b> <math>{}^2J_{Si5-C-H}</math> (9)</p>	—	 <p>-7 -8 -9 -10 -11</p> <p><b>Simulation details</b>  A: <math>\delta</math> -9.5 (N = 1, spin = <math>\frac{1}{2}</math>)  B: <math>\delta</math> 250 (N = 1, spin = <math>\frac{1}{2}</math>)  C: <math>\delta</math> 251 (N = 9, spin = <math>\frac{1}{2}</math>)  <math>J_{A-B}</math> = 0.4 Hz  <math>J_{A-C}</math> = 6 Hz  Decet of doublets</p>

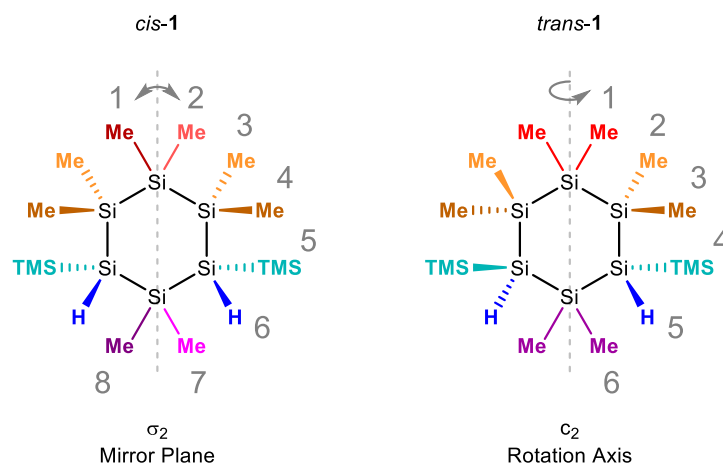


**Figure S3.** Symmetry elements in *cis-1* and *trans-1*. The  $\sigma_v$  mirror plane of *cis-1* gives it  $C_s$  symmetry, whereas *trans-1* is  $C_2$  symmetric. The different symmetry elements result in a different number of chemically inequivalent groups and expected number of  ${}^1H$  NMR peaks.



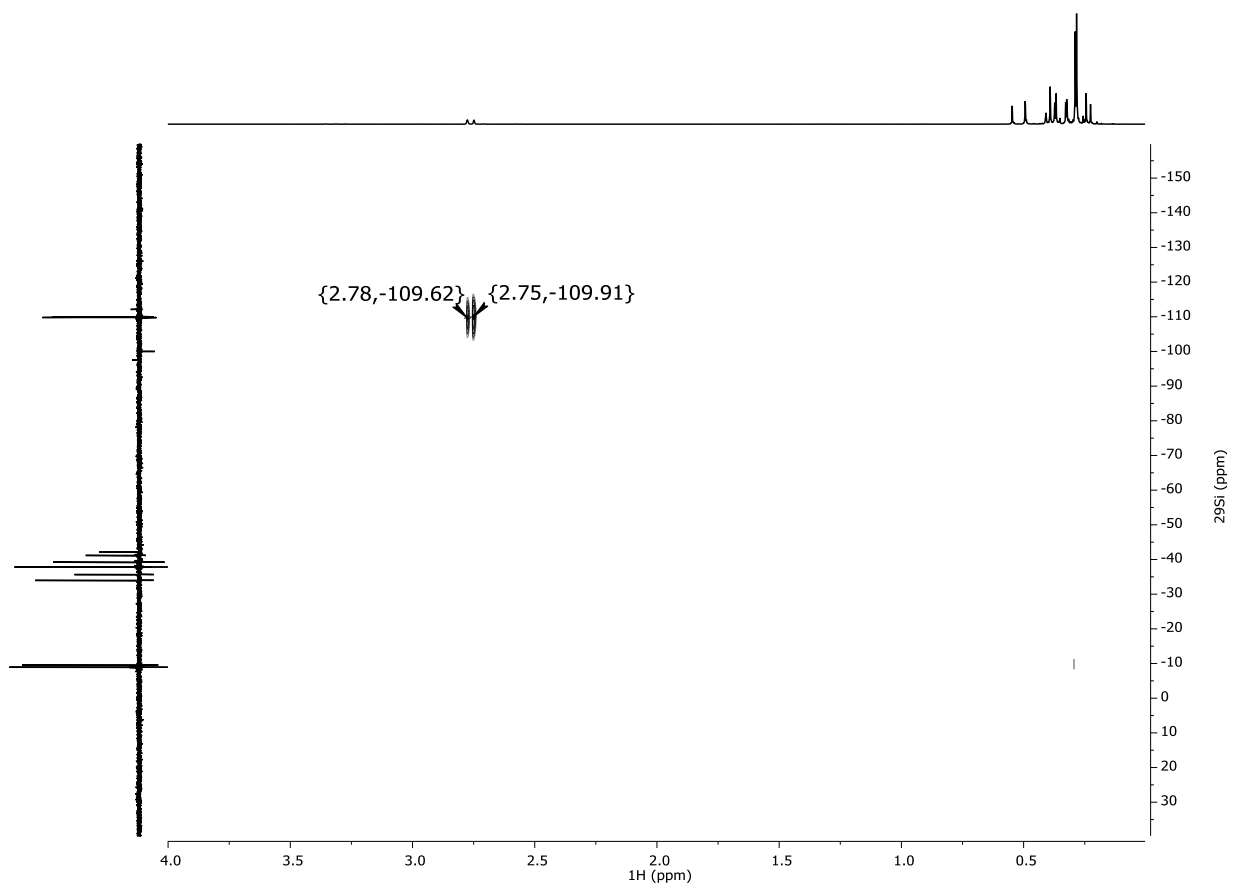


**Figure S-4.**  $^1\text{H}$ - $^{29}\text{Si}$  HSQC (400 MHz,  $\text{C}_6\text{D}_6$ ) spectrum of **1** (55:45 *cis:trans*).  $J_x = 120$  Hz (shows one-bond correlations).

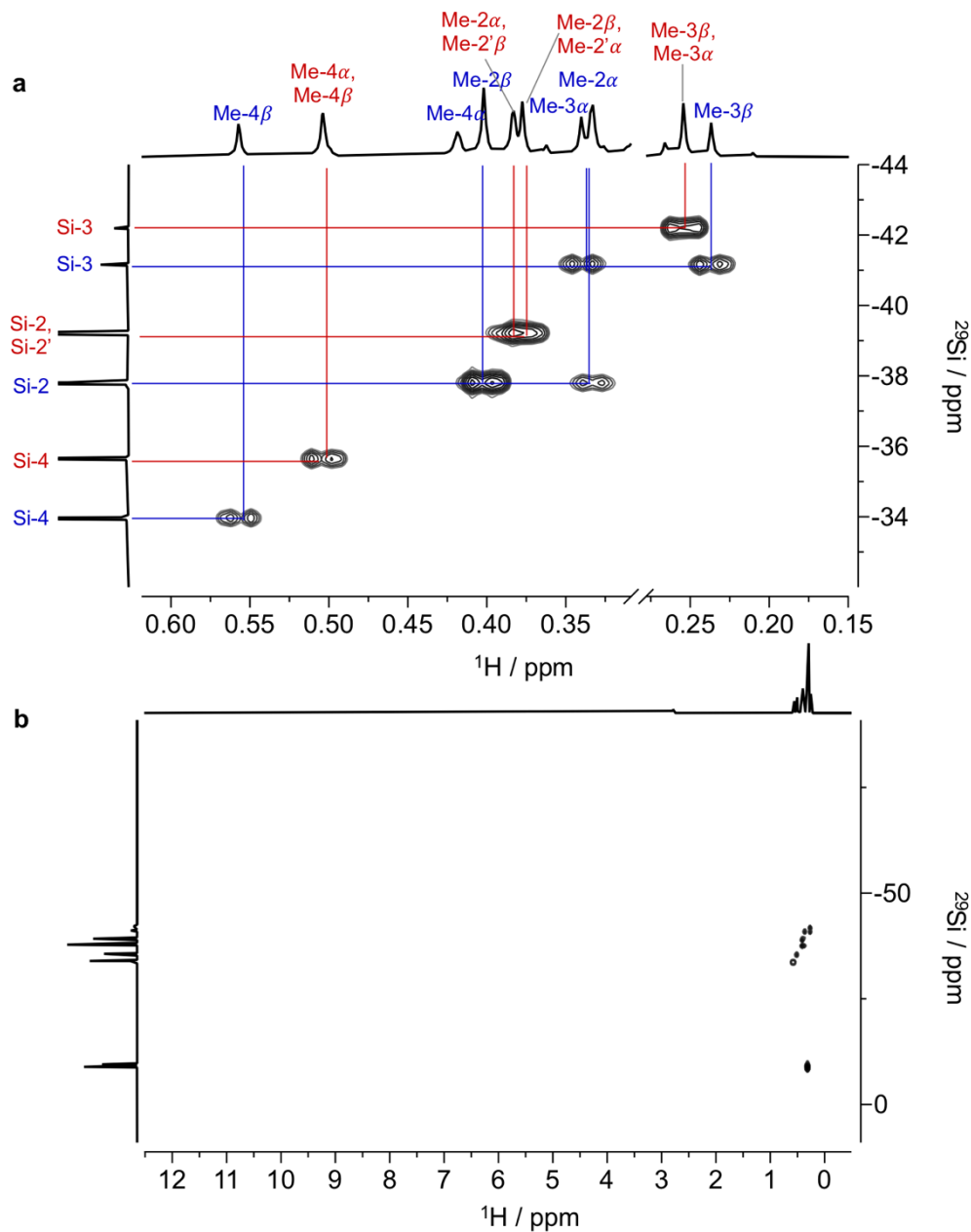


**Figure S-5.** a) Cropped  $^1\text{H}$ - $^{29}\text{Si}$  HMBC (400 MHz,  $\text{C}_6\text{D}_6$ ,  $J_x = 3$  Hz) spectrum of **1** (55:45 cis:trans) highlighting two-bond correlations between Si-2, Si-3, Si-4 and their corresponding methyl groups. Cross-peak between Me-4 $\alpha$  and Si-4 is missing, but appears at other values of  $J_x$  (see Figures S-6, S-7). b) Full  $^1\text{H}$ - $^{29}\text{Si}$  HMBC (400 MHz,  $\text{C}_6\text{D}_6$ ,  $J_x = 3$  Hz) spectrum of **1** (55:45 cis:trans).

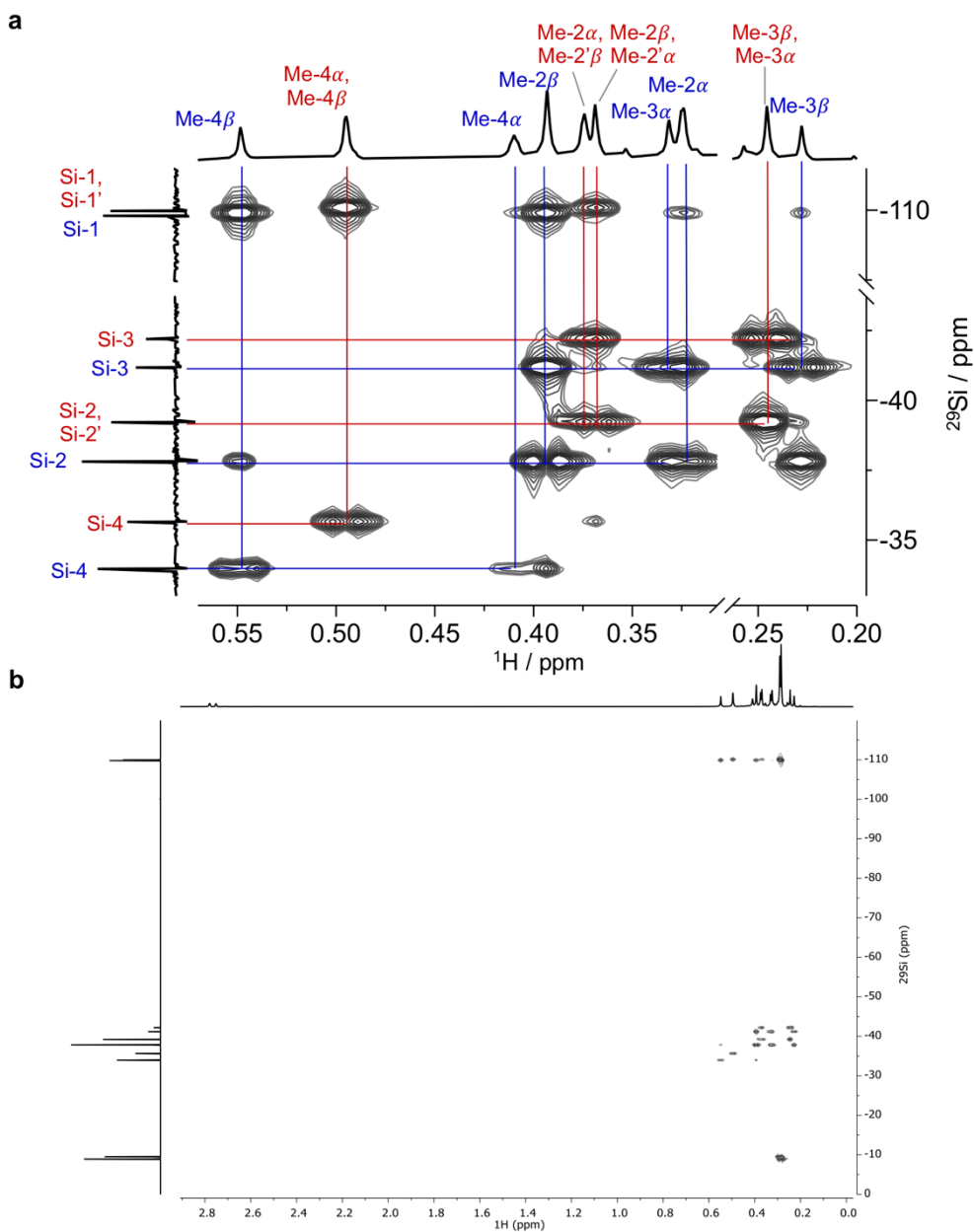


**Figure S-6.** a) Cropped  $^1\text{H}$ - $^{29}\text{Si}$  HMBC (400 MHz,  $\text{C}_6\text{D}_6$ ,  $J_X = 10$  Hz) spectrum of **1** (55:45 cis:trans) highlighting two- and three-bond correlations between Si-2, Si-3, Si-4 and their corresponding methyl groups. b) Full  $^1\text{H}$ - $^{29}\text{Si}$  HMBC (400 MHz,  $\text{C}_6\text{D}_6$ ,  $J_X = 10$  Hz) spectrum of **1** (55:45 cis:trans).

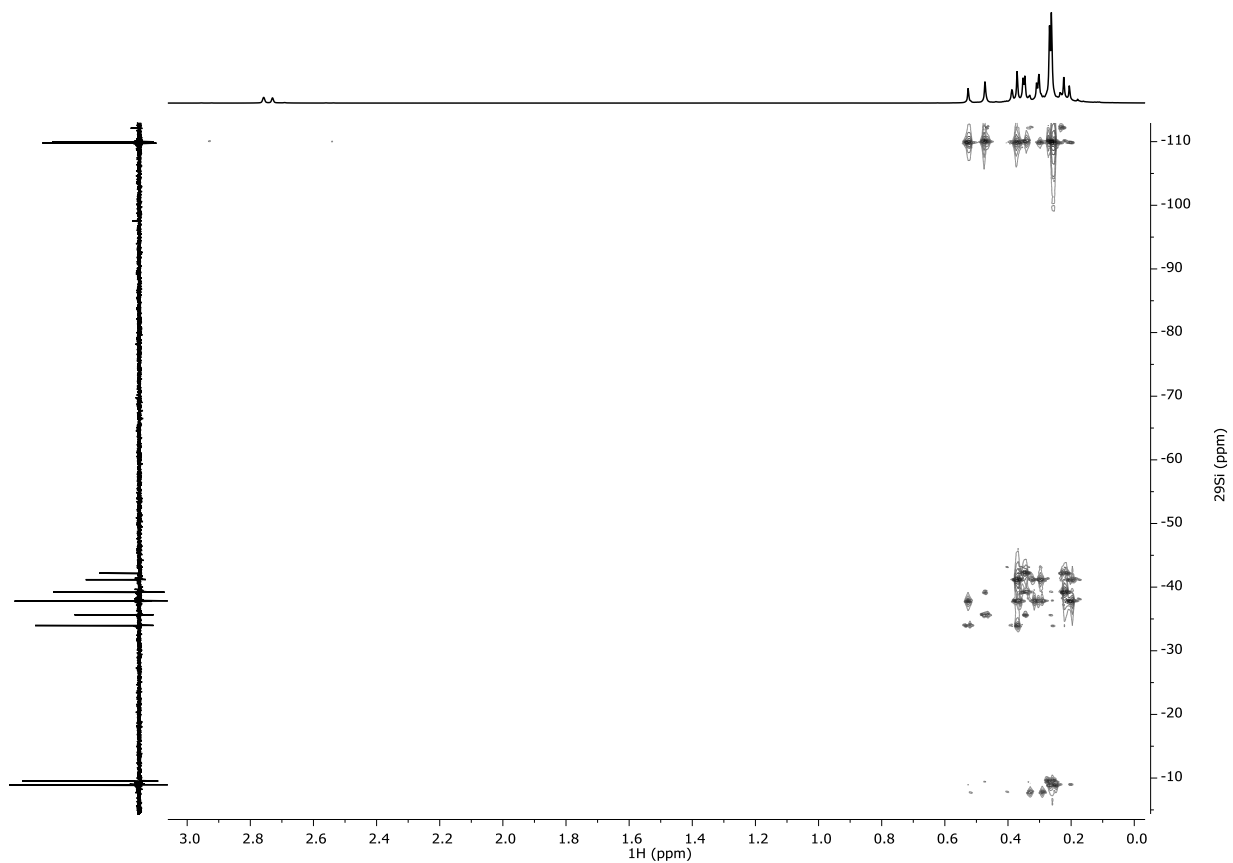


**Figure S-7.** Full  $^1\text{H}$ - $^{29}\text{Si}$  HMBC (400 MHz,  $\text{C}_6\text{D}_6$ ,  $J_x = 7$  Hz) spectrum of **1** (55:45 cis:trans) highlighting two- and three-bond correlations. See Figure 6 in the manuscript for cropped spectrum.

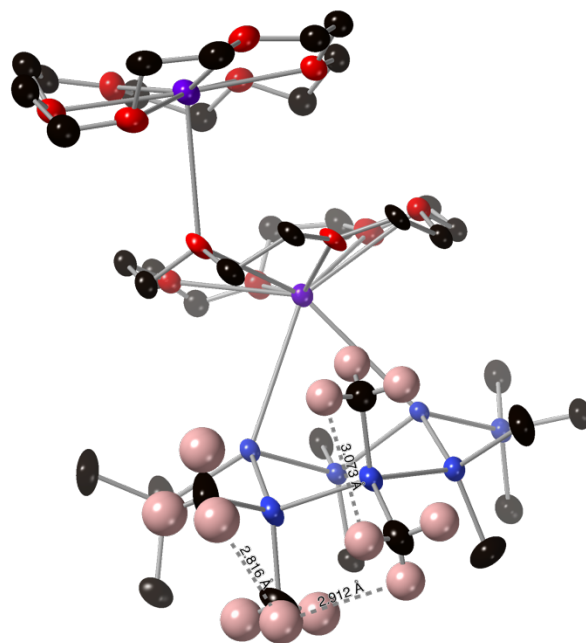


**Figure S-8.** Interproton distances in  $7^{2-} \cdot 2[\text{K}(18\text{-cr-6})]^+$ . Similar interproton distances were observed between protons on methyl groups attached to the same or adjacent silicon atoms. Most hydrogens omitted for clarity. Blue = silicon; black = carbon; red = oxygen; pink = hydrogen; purple = potassium.

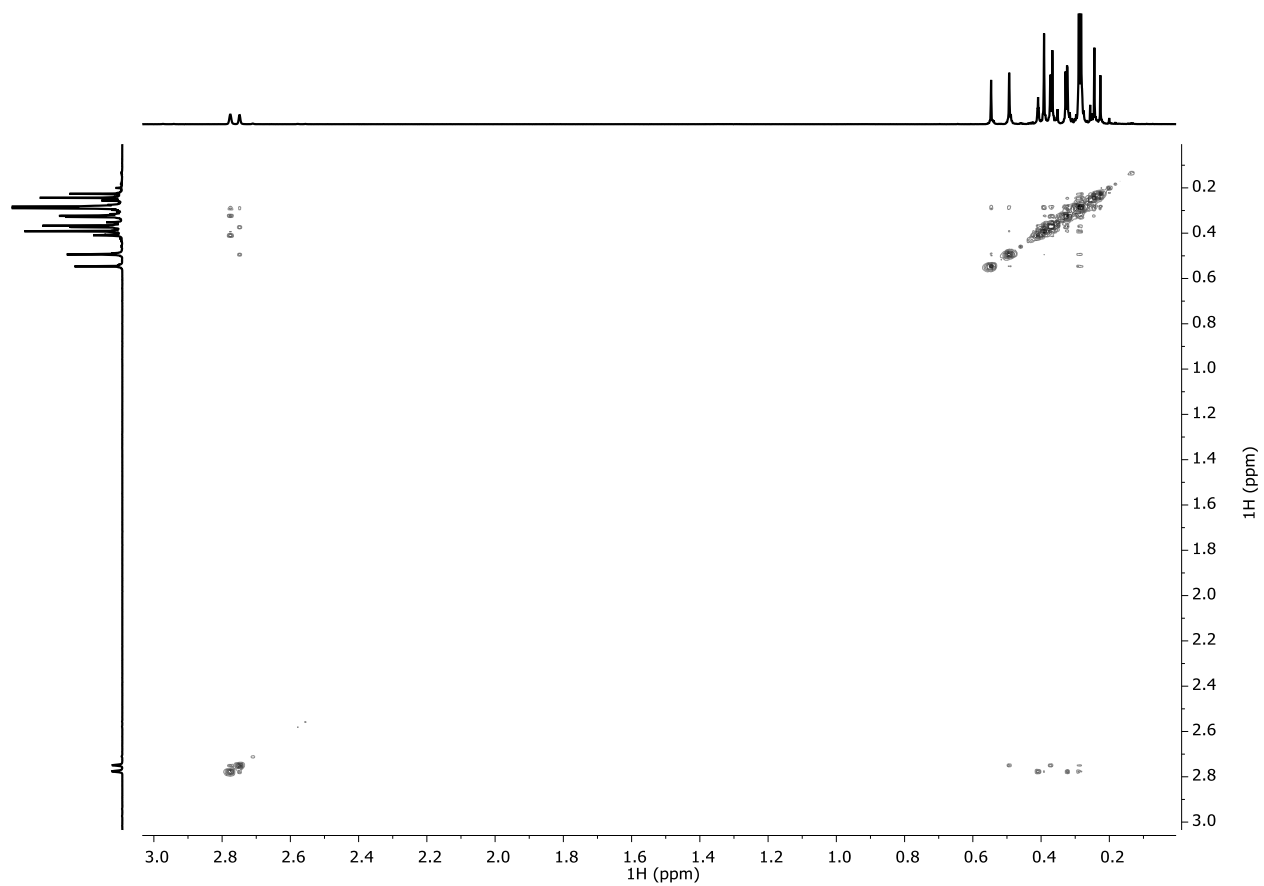


**Figure S-9.** Full <sup>1</sup>H-<sup>1</sup>H gCOSY (400 MHz, C<sub>6</sub>D<sub>6</sub>) spectrum of **1** (55:45 *cis:trans*).

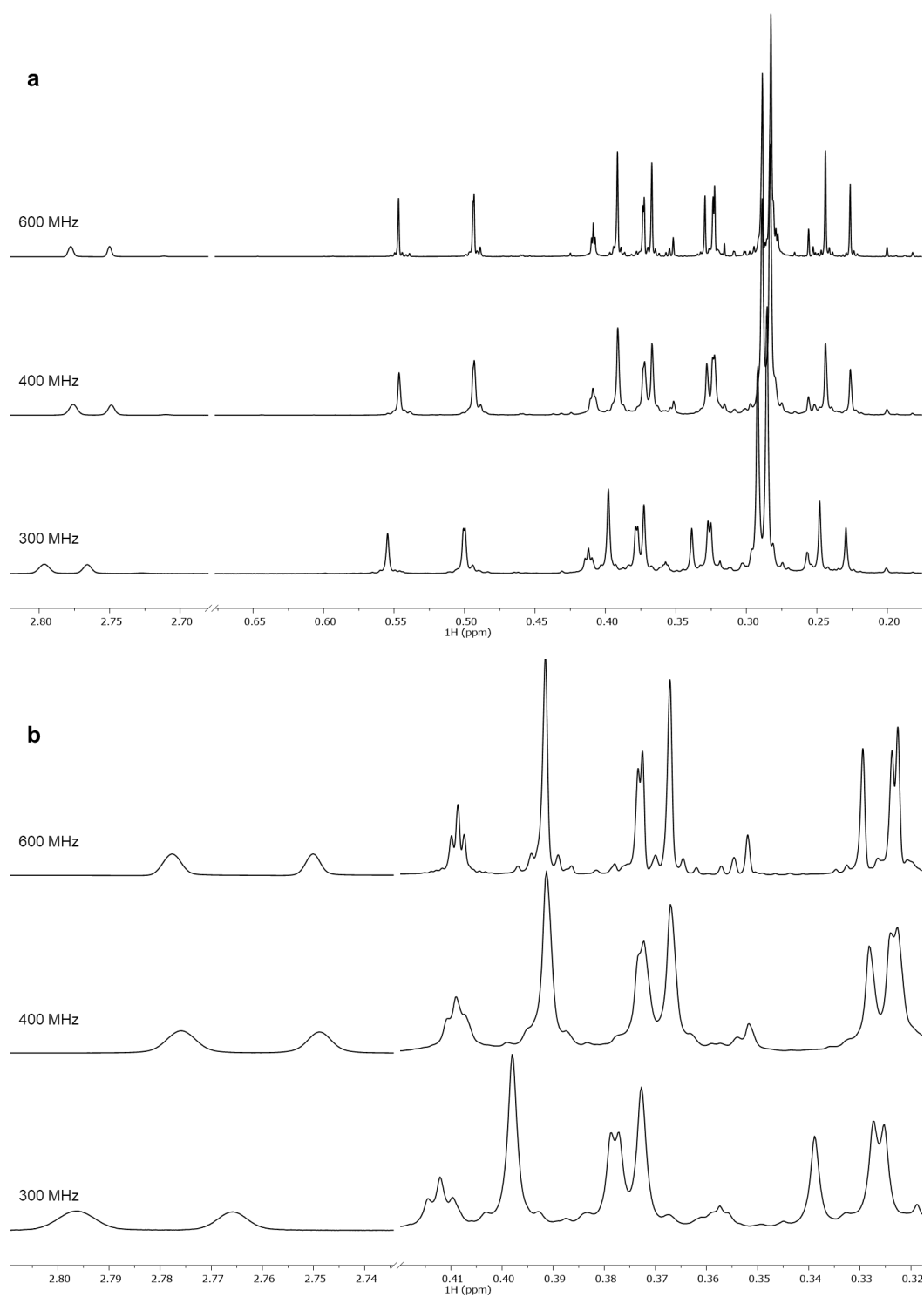


**Figure S-10.**  $^1\text{H}$  NMR spectra of 55:45 *cis:trans* **1** collected on spectrometers of different field strength shown to distinguish coupling constants from chemical shift differences in overlapping peaks.

## 2. NMR Spectra

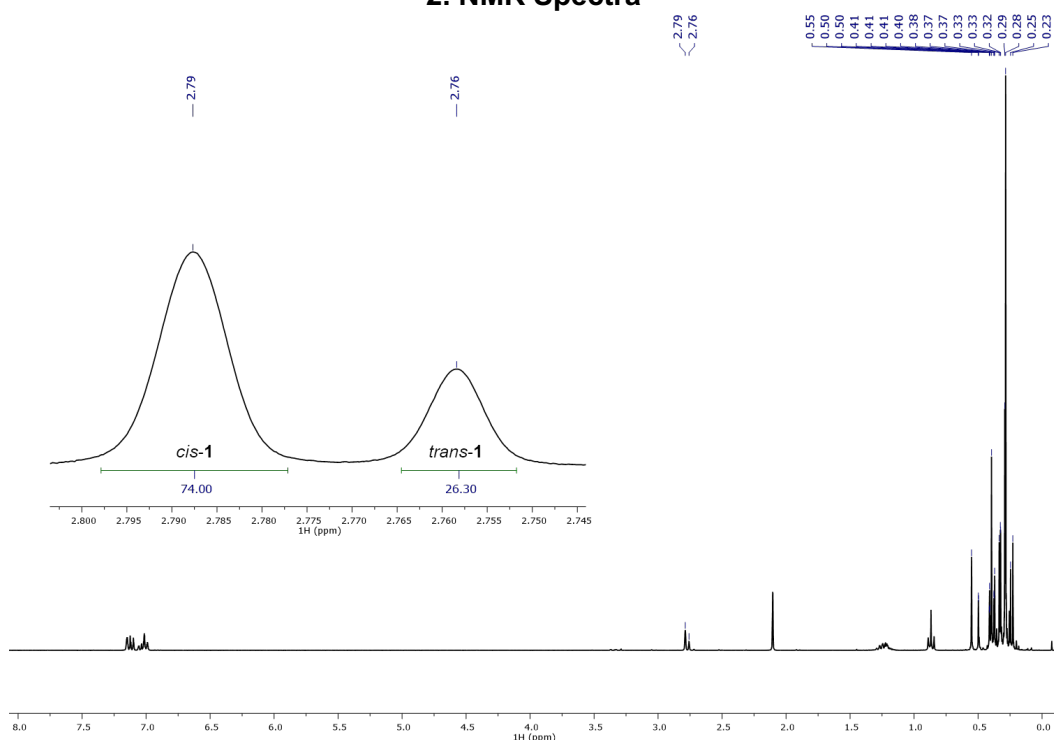


**Figure S-11.**  $^1\text{H}$  NMR (400 MHz,  $\text{C}_6\text{D}_6$ ) spectrum of **1** (74:26 *cis:trans*) including inset with integrals to show relative abundance of isomers.

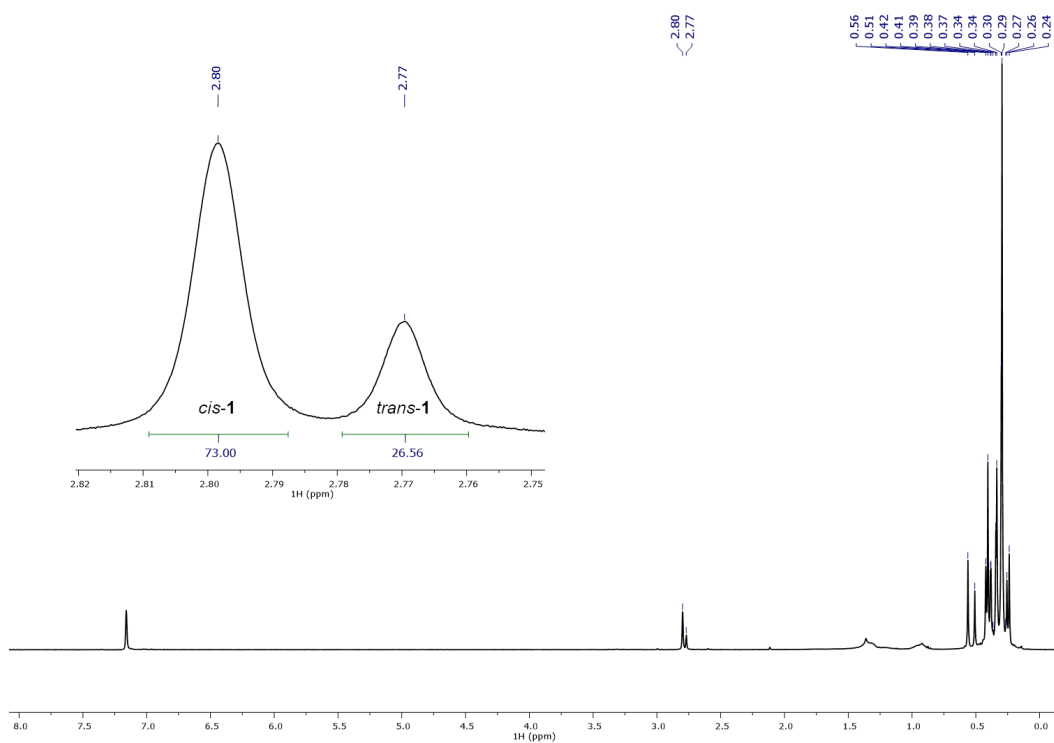


**Figure S-12.**  $^1\text{H}$  NMR (400 MHz,  $\text{C}_6\text{D}_6$ ) spectrum of **1** (73:27 *cis:trans*) including inset with integrals to show relative abundance of isomers.



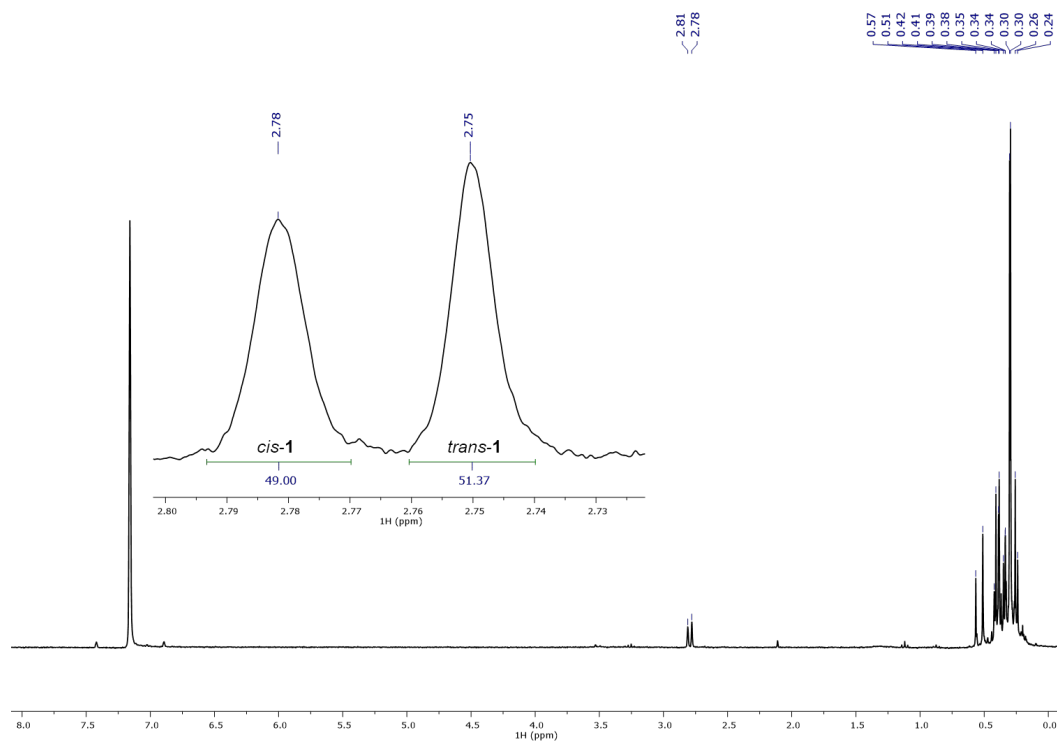


**Figure S-13.**  $^1\text{H}$  NMR (400 MHz,  $\text{C}_6\text{D}_6$ ) spectrum of **1** (49:51 *cis:trans*) including inset with integrals to show relative abundance of isomers.

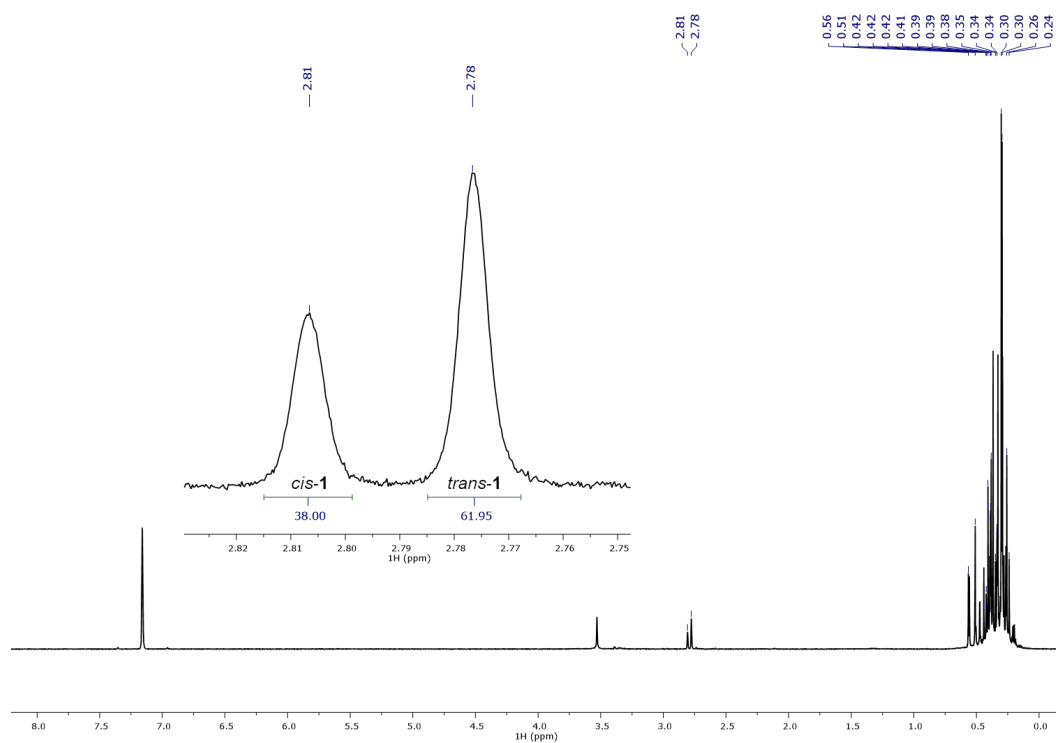


**Figure S-14.**  $^1\text{H}$  NMR (400 MHz,  $\text{C}_6\text{D}_6$ ) spectrum of **1** (38:62 *cis:trans*) including inset with integrals to show relative abundance of isomers.

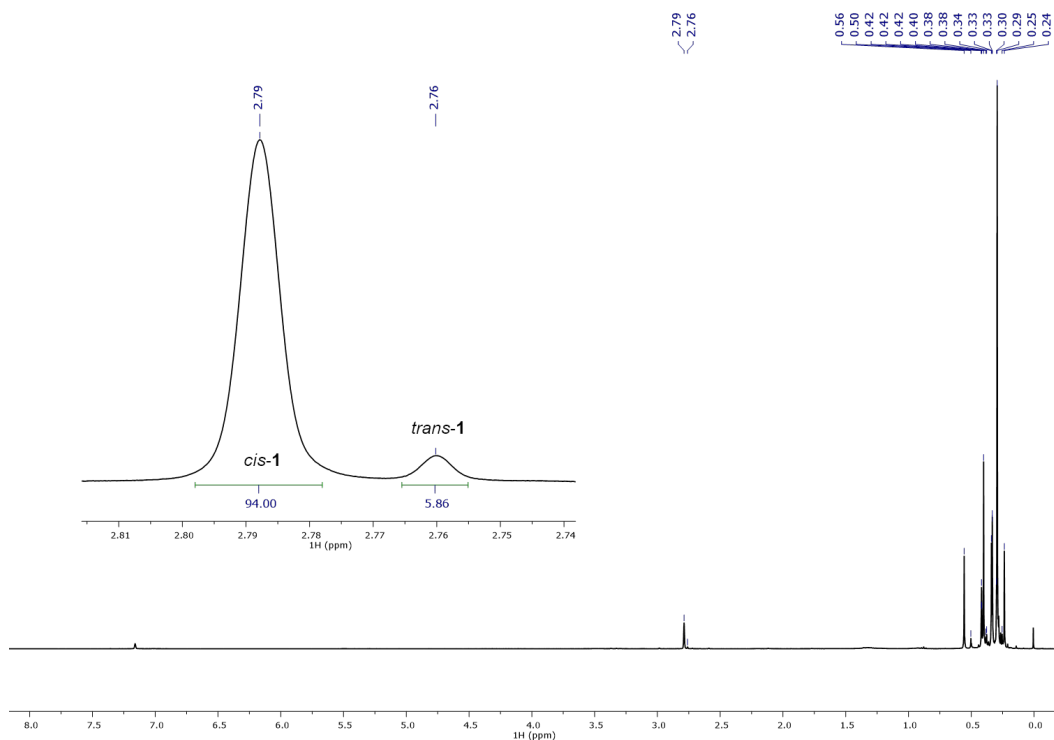


**Figure S-15.**  $^1\text{H}$  NMR (400 MHz,  $\text{C}_6\text{D}_6$ ) spectrum of **1** (94:6 *cis:trans*) including inset with integrals to show relative abundance of isomers.

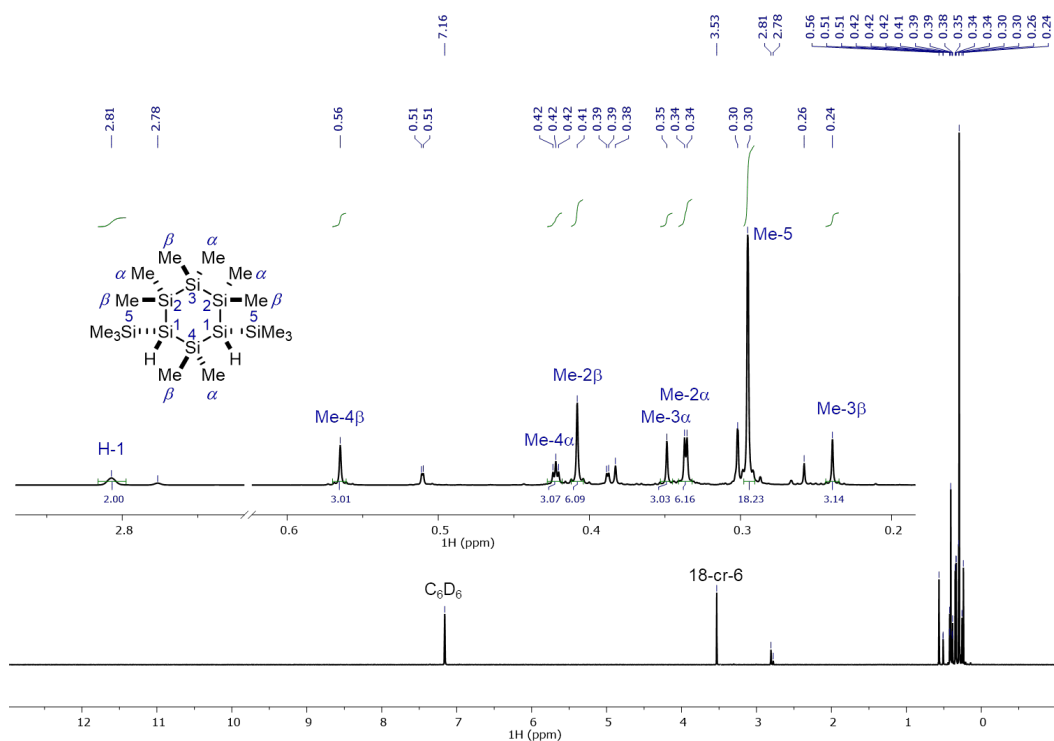


**Figure S-16.**  $^1\text{H}$  NMR (400 MHz,  $\text{C}_6\text{D}_6$ ) spectrum of **1** (83:17 *cis:trans*) with assignments shown for *cis*-**1**.

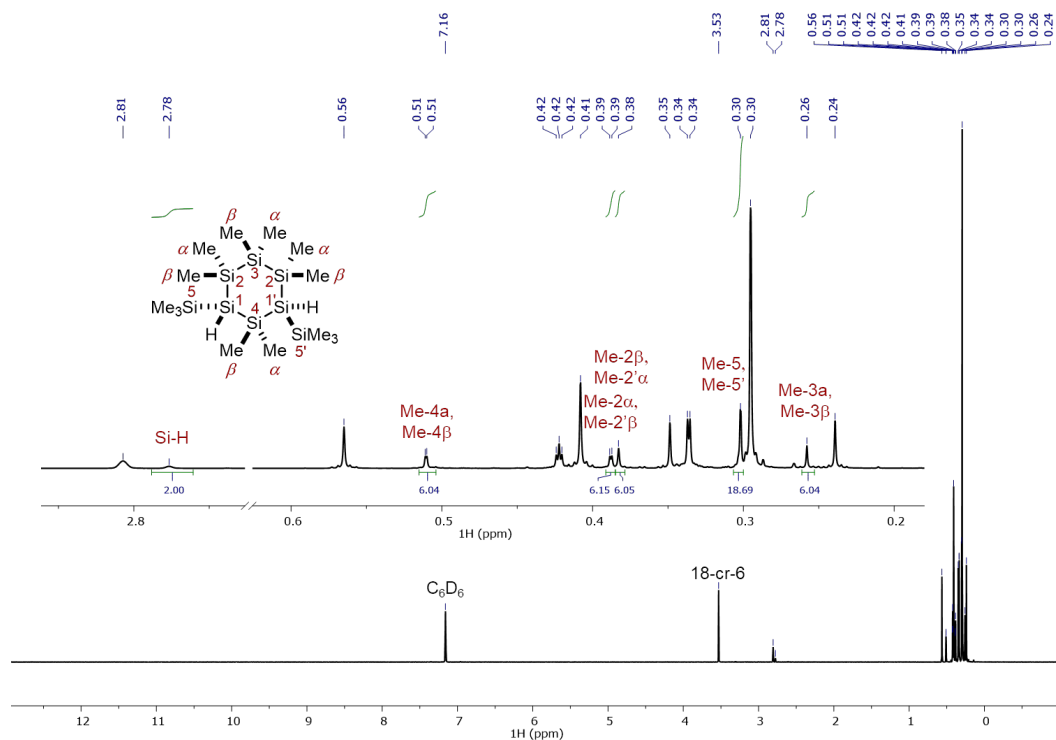


**Figure S-17.**  $^1\text{H}$  NMR (400 MHz,  $\text{C}_6\text{D}_6$ ) spectrum of **1** (83:17 *cis:trans*) with assignments shown for *trans-1*.

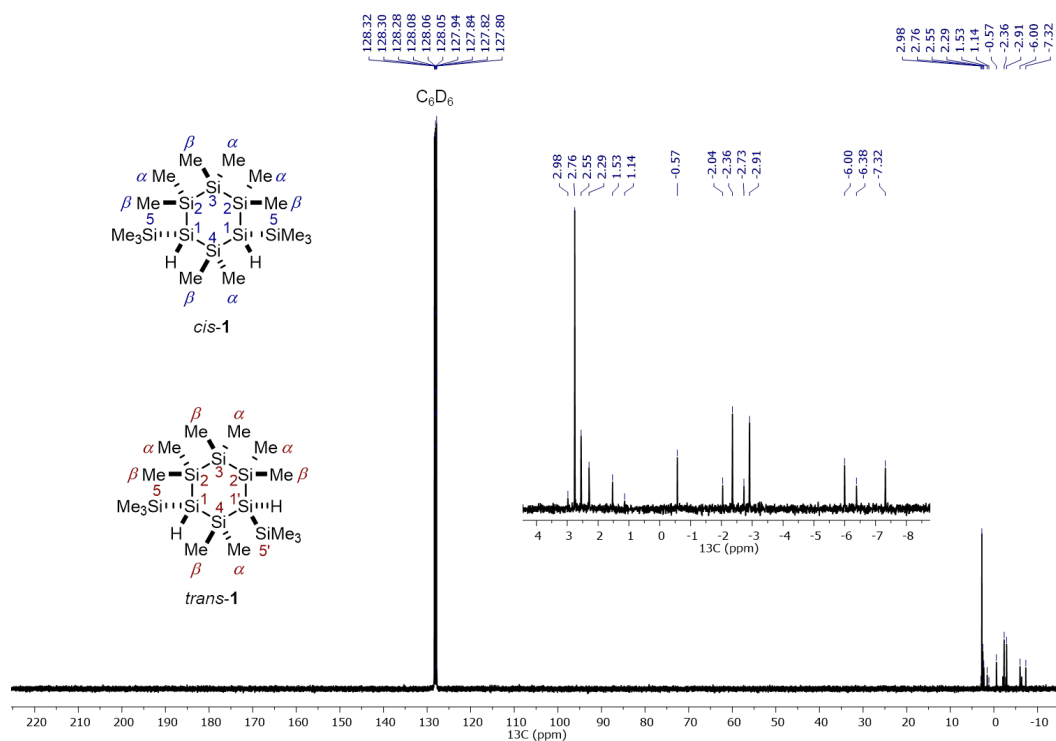


**Figure S-18.**  $^{13}\text{C}$   $\{^1\text{H}\}$  NMR spectrum (101 MHz,  $\text{C}_6\text{D}_6$ ) of (83:17 *cis:trans*) **1**. Inset shows methyl region for clarity.

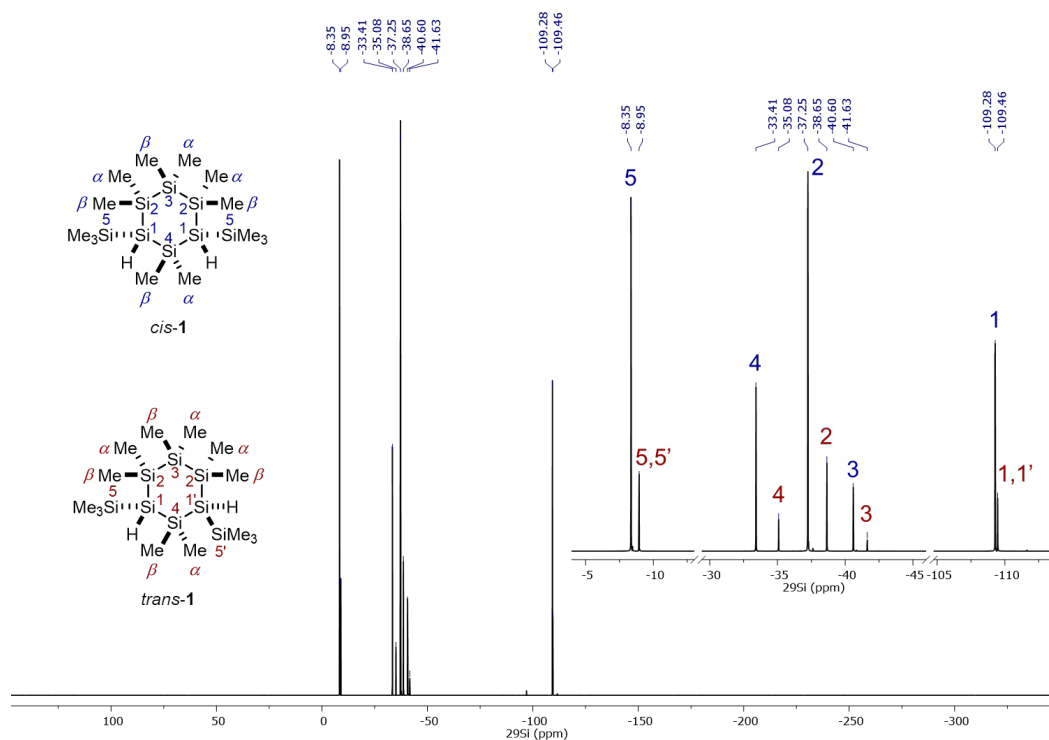


**Figure S-19.**  $^{29}\text{Si} \{^1\text{H}\}$  DEPT 45 NMR (79 MHz,  $\text{C}_6\text{D}_6$ ) spectrum of **1** (83:17 *cis:trans*). Inset shows assignments.

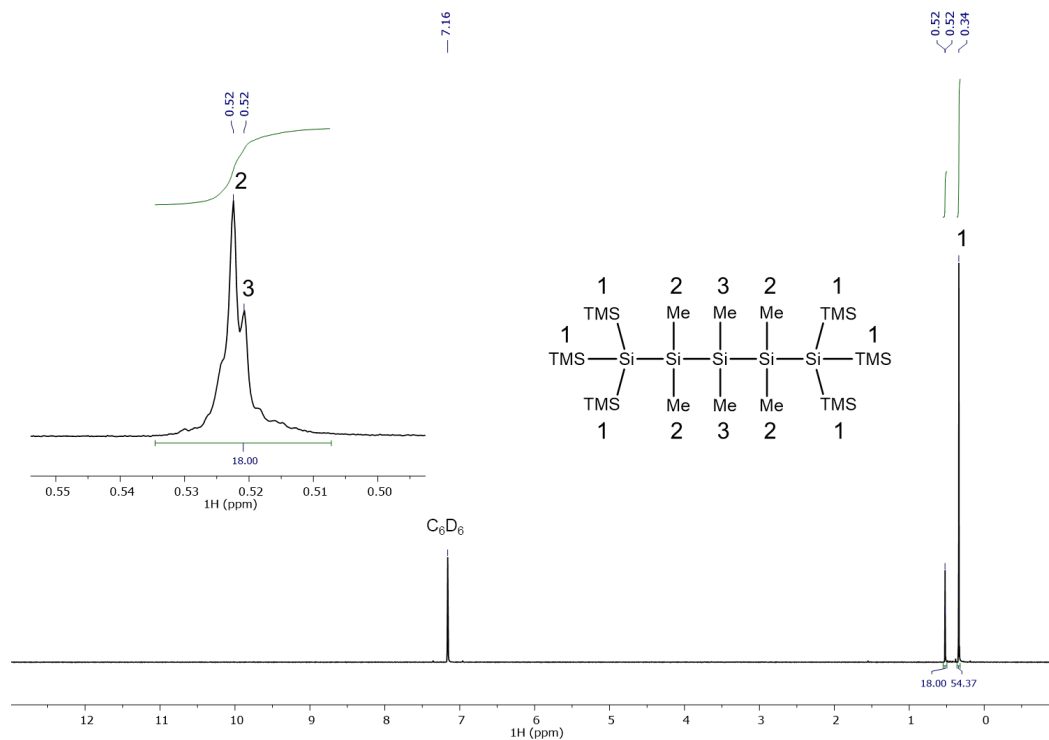


**Figure S-20.**  $^1\text{H}$  NMR (400 MHz,  $\text{C}_6\text{D}_6$ ) spectrum of **4**.

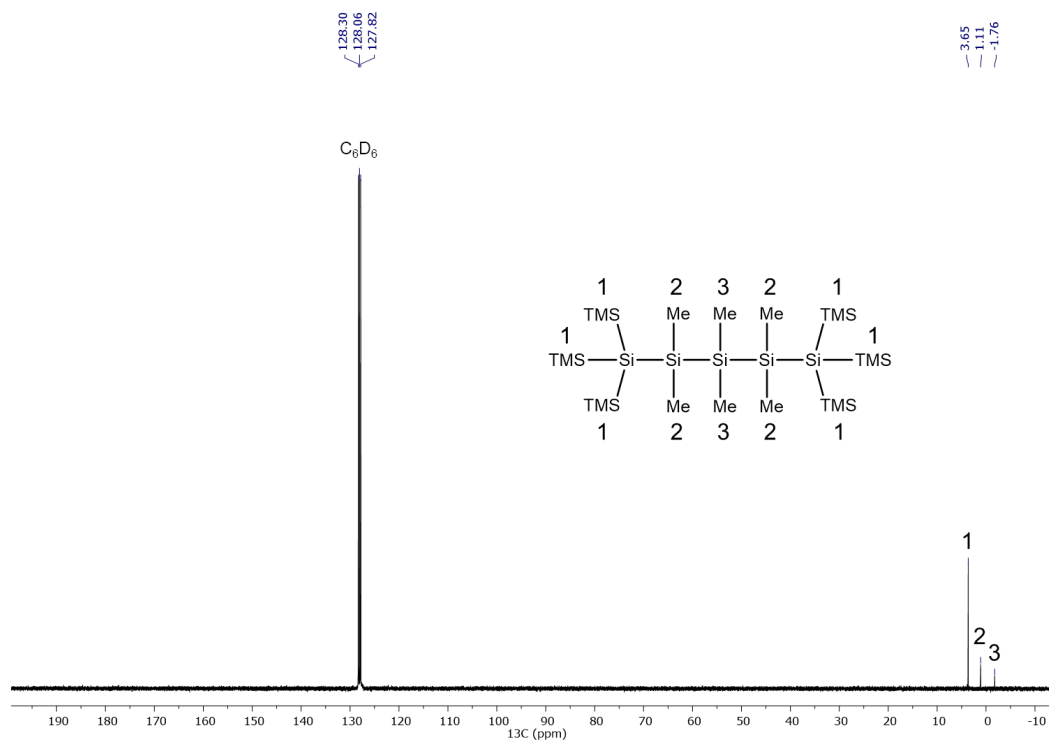


Figure S-21.  $^{13}\text{C}$   $\{^1\text{H}\}$  NMR (101 MHz,  $\text{C}_6\text{D}_6$ ) spectrum of **4**.

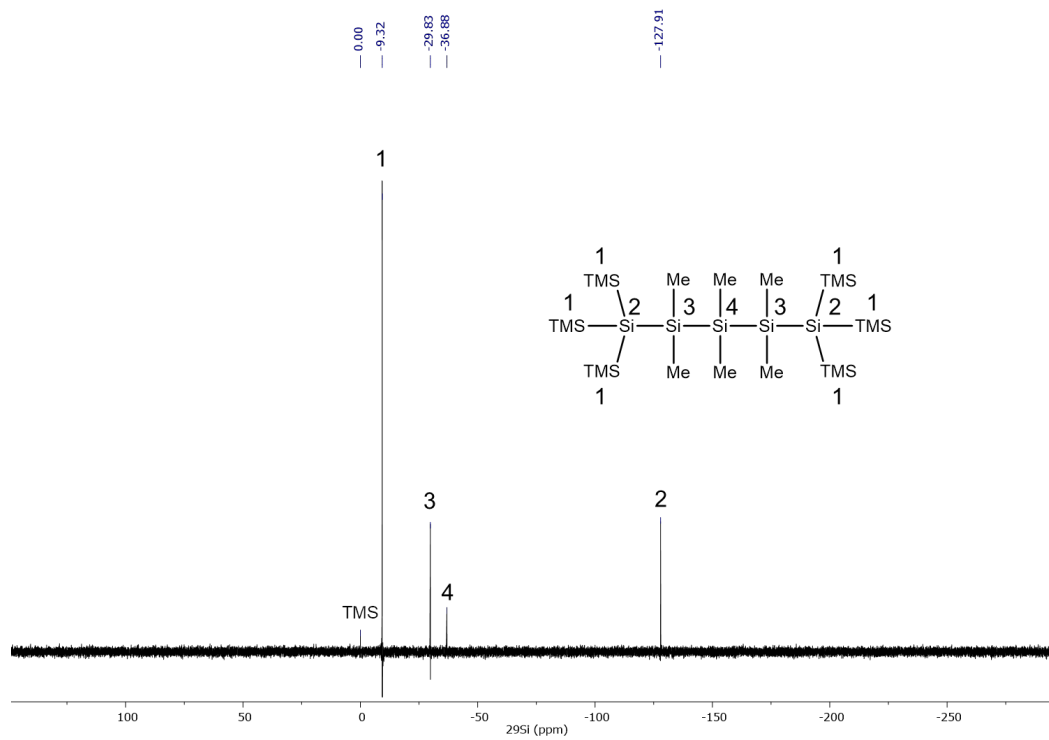
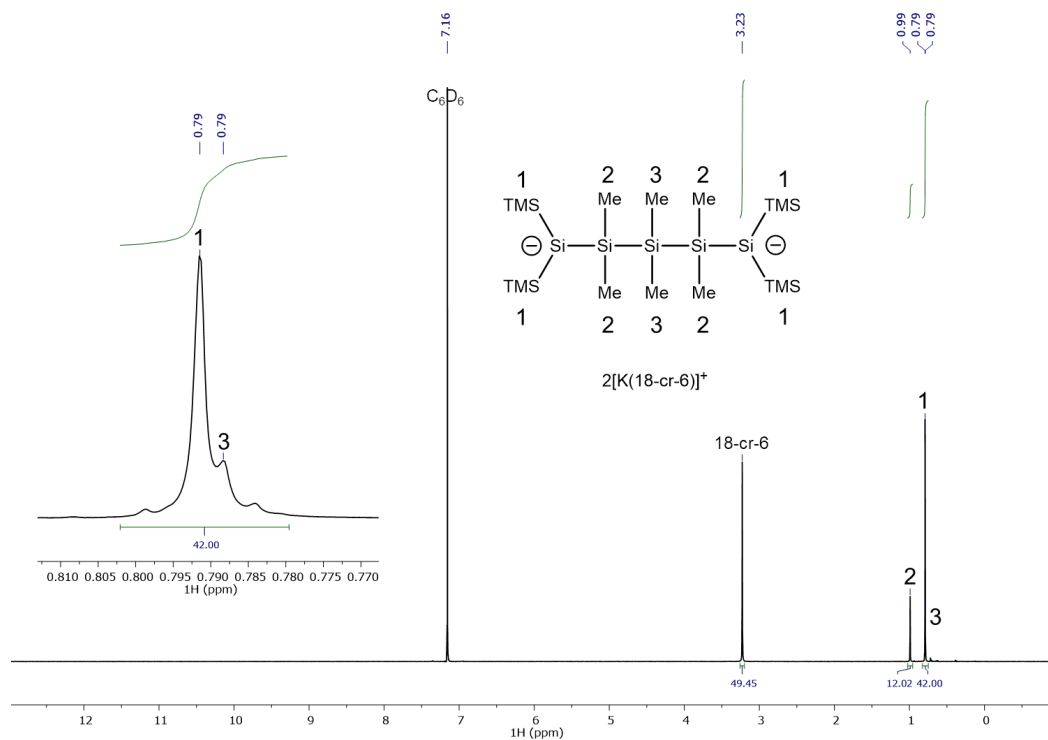
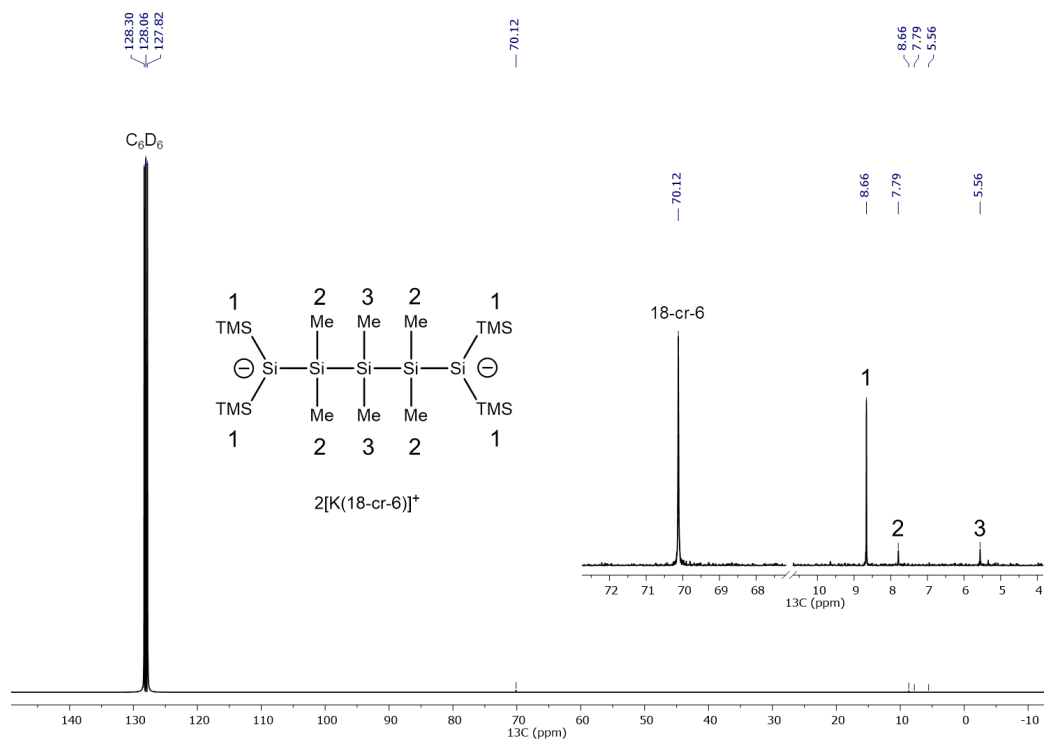


Figure S-22.  $^{29}\text{Si}$   $\{^1\text{H}\}$  DEPT 45 NMR spectrum (79 MHz,  $\text{C}_6\text{D}_6$ ) of **4**.



**Figure S-23.**  $^1\text{H}$  NMR spectrum (400 MHz,  $\text{C}_6\text{D}_6$ ) of  $5^{2-}\cdot 2[\text{K}(18\text{-cr-6})]^+$ .



**Figure S-24.**  $^{13}\text{C}$   $\{^1\text{H}\}$  NMR spectrum (101 MHz,  $\text{C}_6\text{D}_6$ ) of  $5^{2-}\cdot 2[\text{K}(18\text{-cr-6})]^+$ .

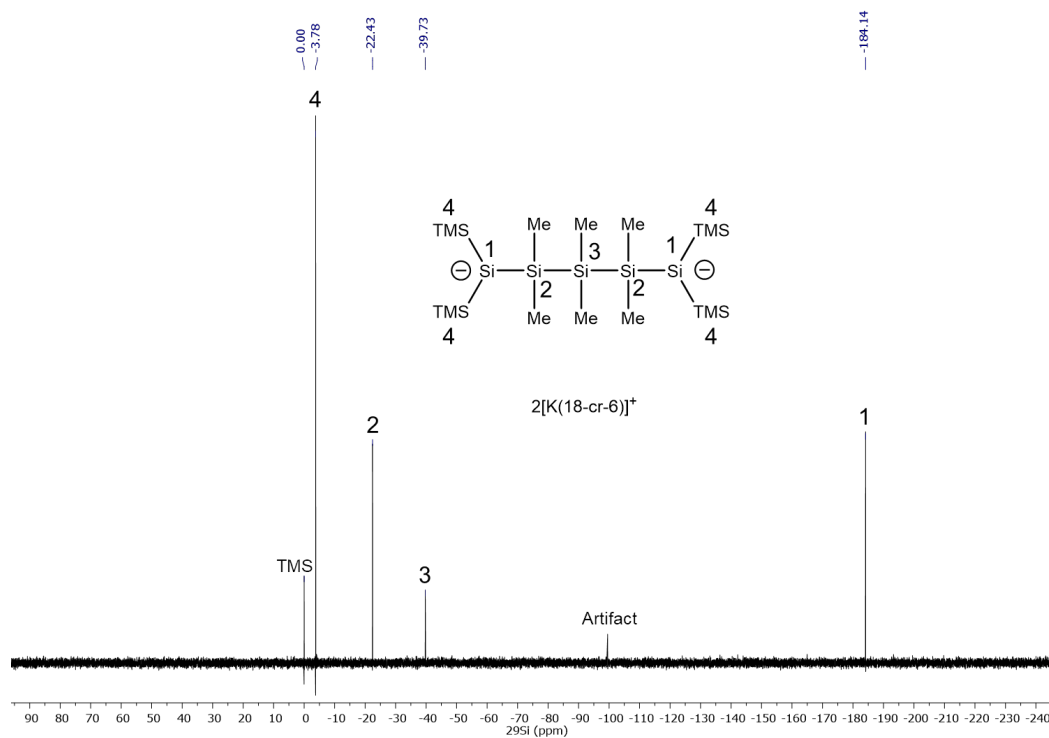


**Figure S-25.**  $^{29}\text{Si} \{^1\text{H}\}$  DEPT 45 NMR spectrum (79 MHz,  $\text{C}_6\text{D}_6$ ) of  $5^{2-} \cdot 2[\text{K}(18\text{-cr-6})]^+$ .

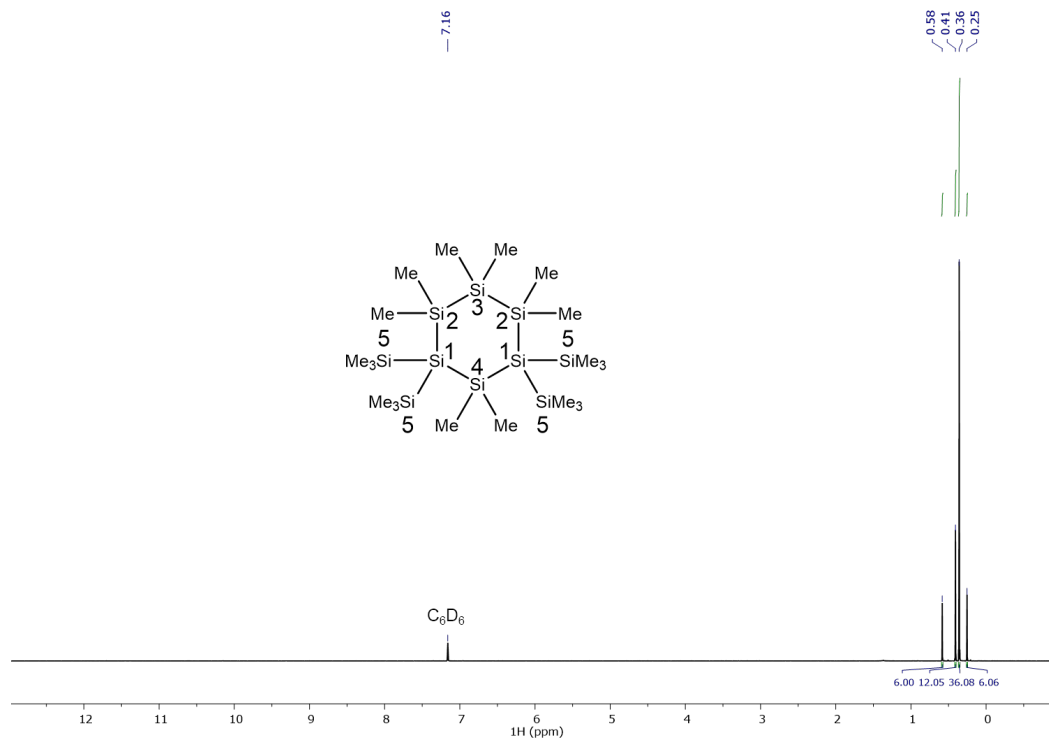


**Figure S-26.**  $^1\text{H}$  NMR (400 MHz,  $\text{C}_6\text{D}_6$ ) spectrum of **6**.

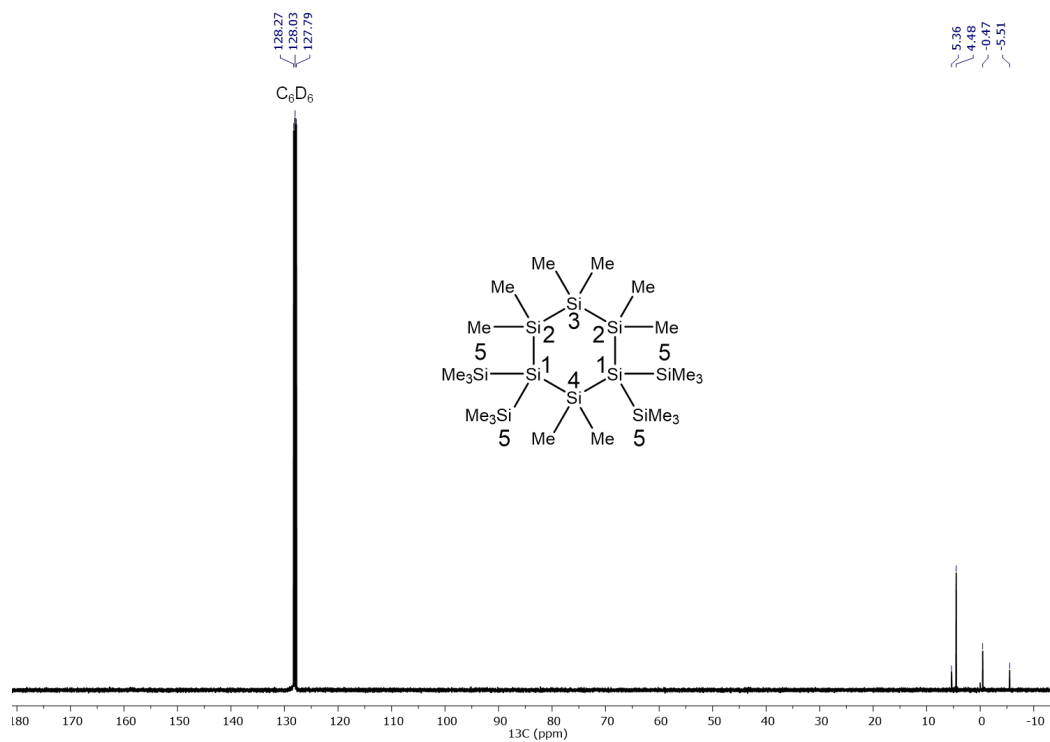


Figure S-27.  $^{13}\text{C}$   $\{^1\text{H}\}$  NMR (101 MHz,  $\text{C}_6\text{D}_6$ ) spectrum of **6**.

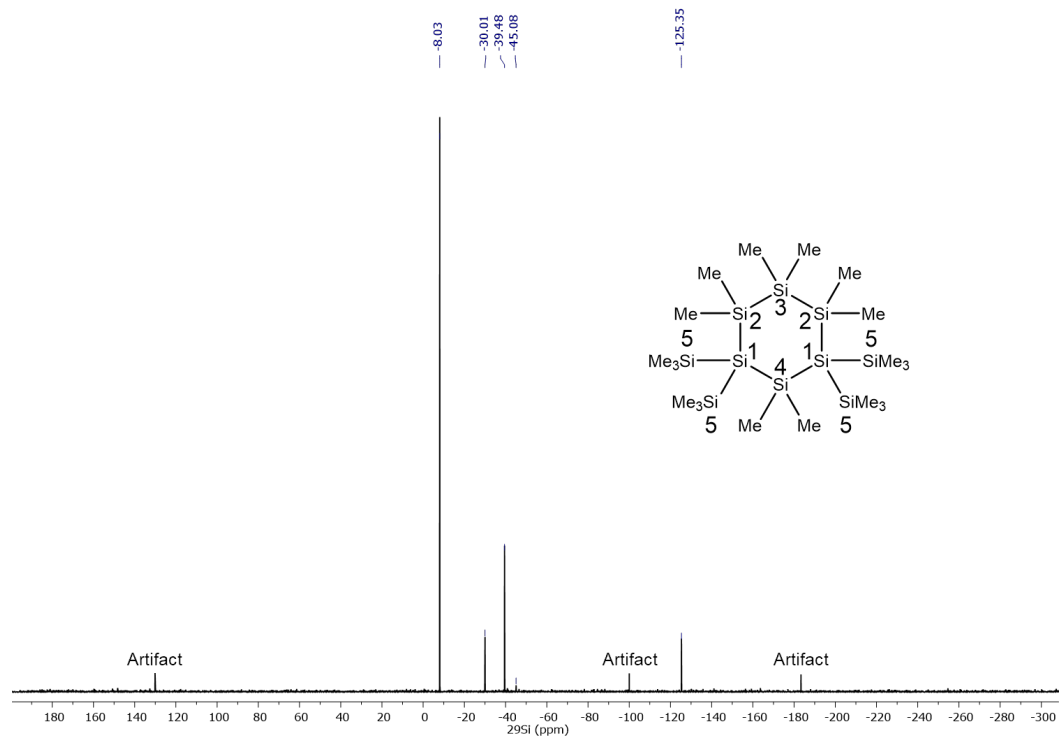


Figure S-28.  $^{29}\text{Si}$   $\{^1\text{H}\}$  DEPT 45 NMR (79 MHz,  $\text{C}_6\text{D}_6$ ) spectrum of **6**.



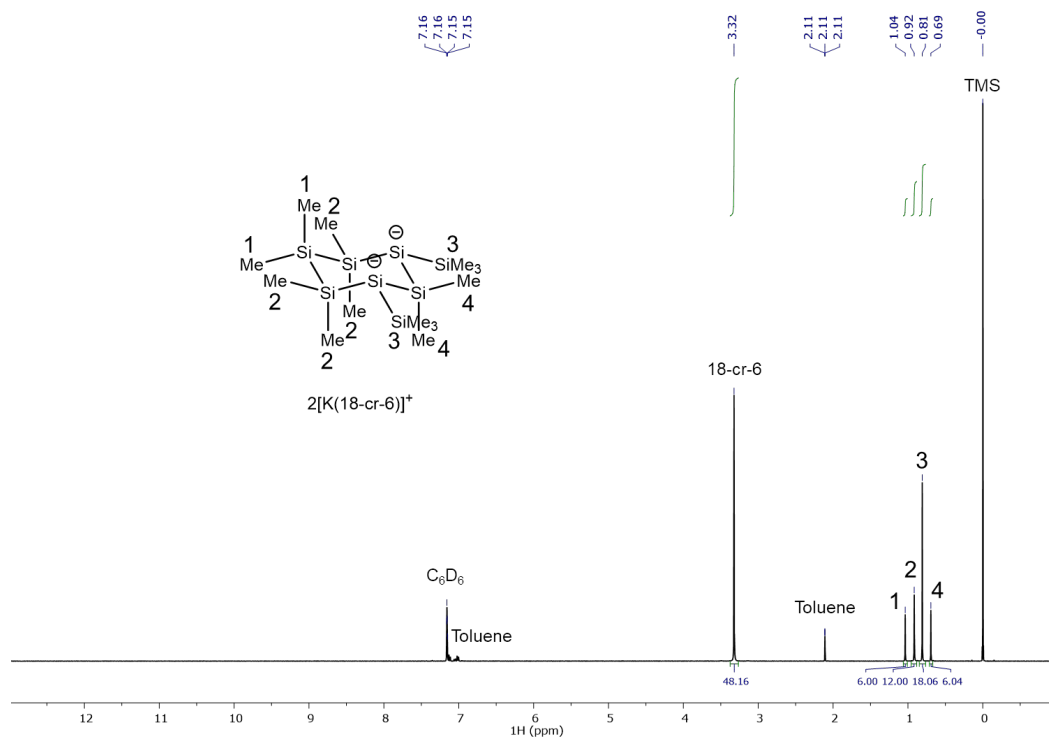


Figure S-29.  $^1\text{H}$  NMR (400 MHz,  $\text{C}_6\text{D}_6$ ) spectrum of 7.

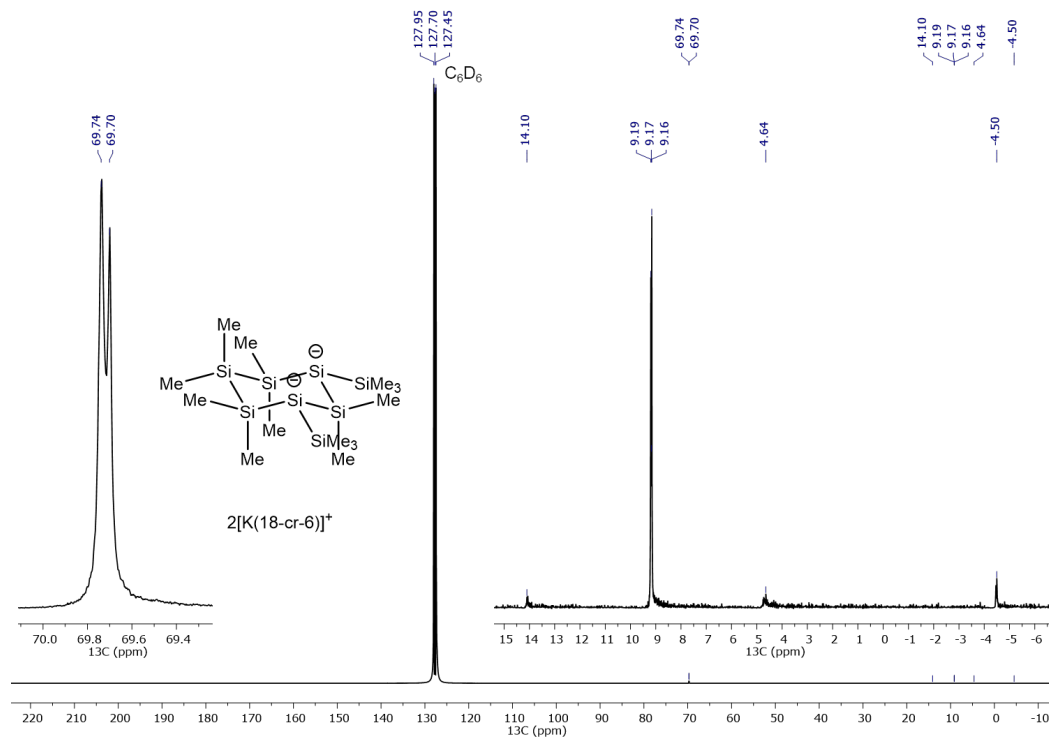
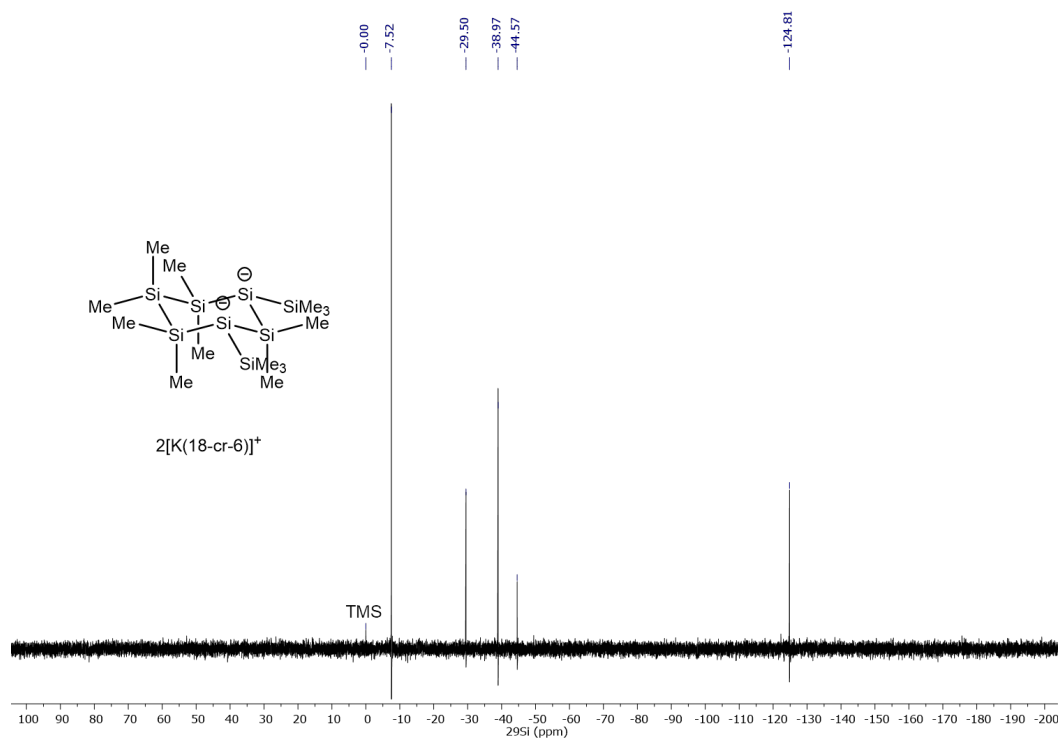


Figure S-30.  $^{13}\text{C}$   $\{^1\text{H}\}$  NMR (101 MHz,  $\text{C}_6\text{D}_6$ ) spectrum of 7.



**Figure S-31.**  $^{29}\text{Si}$  { $^1\text{H}$ } DEPT 45 NMR (79 MHz,  $\text{C}_6\text{D}_6$ ) spectrum of **7**.

### 3. Single Crystal X-Ray Crystallographic Data

#### Single Crystal X-ray Crystallography

All reflection intensities were measured at 110(2) K for compounds **4** and **7**, at 130(2) K for compound **5**,\* and at 200(2) K for compound **6**.\*\* Data were collected using a SuperNova diffractometer (equipped with Atlas detector) either with Mo  $K\alpha$  radiation ( $\lambda = 0.71073 \text{ \AA}$ ) for **5**, **6** and **7** or with Cu  $K\alpha$  radiation ( $\lambda = 1.54178 \text{ \AA}$ ) for **4** under the program CrysAlisPro (Version CrysAlisPro 1.171.39.29c, Rigaku OD, 2017). The same program was used to refine the cell dimensions and for data reduction. The structure was solved with the program SHELXS-2014/7 or SHELXS-2018/3 (Sheldrick, 2015) and was refined on  $F^2$  with SHELXL-2014/7 or SHELXS-2018/3 (Sheldrick, 2015). For **4**, analytical numeric absorption correction using a multifaceted crystal model was applied using CrysAlisPro. For **5**, **6**, and **7**, numerical absorption correction based on gaussian integration over a multifaceted crystal model was applied using CrysAlisPro. The temperature of the data collection was controlled using the system Cryojet (manufactured by Oxford Instruments). The H atoms were placed at calculated positions using the instructions AFIX 23, AFIX 43 or AFIX 137 with isotropic displacement parameters having values 1.2 or 1.5  $U_{\text{eq}}$  of the attached C atoms.

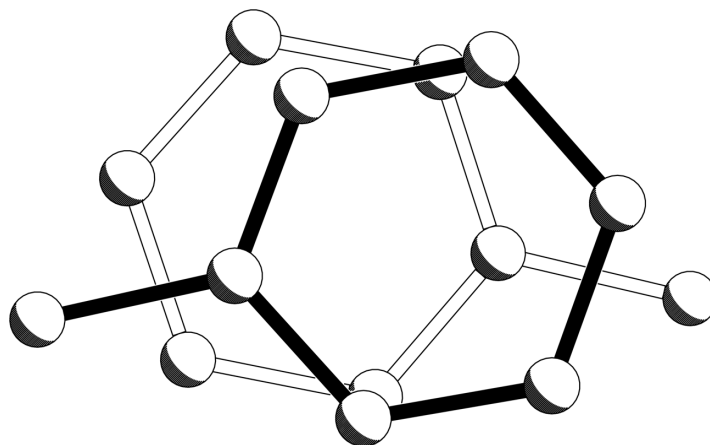
\* At 110 K, the crystal that was mounted on the diffractometer appeared to suffer from significant crystal damage, and the diffraction pattern showed a significant amount of split reflections. At 130 K, another crystal remained single, and the diffraction pattern showed no split reflections. Crystals of compound **4** are air sensitive, and crystal damage occurs rapidly when exposed to air. In order to keep the integrity of the crystals prior mounting, crystals were promptly deposited on a microscope slide with Parabar 10312 oil (Paratone) under a cold  $\text{N}_2(\text{g})$  stream in order to minimize crystal decomposition prior mounting the crystal on the diffractometer.

\*\* Upon cooling to ca. 165 K, significantly crystal damage occurred, which is most likely due to a partially destructive solid-solid phase transition, and data were of poor quality. Upon cooling to 200 K, the crystals remained stable, and data could be collected from a single crystal.

#### Additional refinement details

**4:** The structure is ordered. The crystal that was mounted on the diffractometer was twinned, and the two twin components are related by a twofold rotational axis along the reciprocal axis  $\mathbf{c}^*$ . The structure refinement was carried out using the HKLF 5 instruction. The BASF scale factor refines to 0.1670(15). The  $R1 / wR2$  factors are relatively high because data integration was complex. In fact, it was difficult to find a data collection strategy that minimizes overlap between reflections found along the  $\mathbf{c}^*$  direction as the  $c$  dimension is very long (ca. 58  $\text{\AA}$ ). Furthermore, the crystals were all twinned as at least two (or more than two) thin plates were stacked on top of the other. Evidence of twinning is shown from the reciprocal lattice slices down  $\mathbf{a}^*$  and  $\mathbf{b}^*$ .

**5:** The structure is partly disordered. The two 18-crown-6 ligands, and one trimethylsilyl group are disordered over two orientations. The occupancy factors of the major components of the disorder refine to 0.9112(15), 0.745(3), and 0.64(3), respectively. The asymmetric unit also contains one disordered lattice toluene molecule, which is found near K1(18Crown6) (C7S' from the minor component of the disorder is found very near K1). The two orientations of the disorder are shown below (the occupancy factor of the major component of the disorder refines to 0.778(4)).



**6:** The structure is ordered.

**7:** The structure is partly disordered. The two 18C6 molecules are disordered over three orientations. All occupancy factors can be retrieved from the .cif file. The asymmetric unit also contains two lattice toluene solvent molecules. One solvent molecule is found at no special position, and is disordered over two orientations. The occupancy factor of the major component of the disorder refines to 0.826(4). The other solvent molecule is found at one site of inversion symmetry, and the occupancy factor is constrained to 0.5.

**Table S1. Crystallographic data for 4**

	<b>4</b>
Crystal data	
Chemical formula	C <sub>24</sub> H <sub>72</sub> Si <sub>11</sub>
<i>M<sub>r</sub></i>	669.80
Crystal system, space group	Monoclinic, <i>C2/c</i>
Temperature (K)	110
<i>a</i> , <i>b</i> , <i>c</i> (Å)	15.5781 (3), 9.86896 (16), 57.967 (3)
β (°)	96.152 (3)
<i>V</i> (Å <sup>3</sup> )	8860.5 (5)
<i>Z</i>	8
Radiation type	Cu <i>K</i> α
μ (mm <sup>-1</sup> )	3.15
Crystal size (mm)	0.35 × 0.18 × 0.03
Data collection	
Diffractometer	SuperNova, Dual, Cu at zero, Atlas
Absorption correction	Analytical <i>CrysAlis PRO</i> 1.171.39.29c (Rigaku Oxford Diffraction, 2017) Analytical numeric absorption correction using a multifaceted crystal model based on expressions derived by R.C. Clark & J.S. Reid. (Clark, R. C. & Reid, J. S. (1995). <i>Acta Cryst.</i> A51, 887-897) Empirical absorption correction using spherical harmonics, implemented in <i>SCALE3 ABSPACK</i> scaling algorithm.
<i>T<sub>min</sub></i> , <i>T<sub>max</sub></i>	0.507, 0.927
No. of measured, independent and observed [ <i>I</i> > 2σ( <i>I</i> )] reflections	28236, 7889, 7677
<i>R<sub>int</sub></i>	0.049
(sin θ/λ) <sub>max</sub> (Å <sup>-1</sup> )	0.598
Refinement	
<i>R</i> [ <i>F</i> <sup>2</sup> > 2σ( <i>F</i> <sup>2</sup> )], <i>wR</i> ( <i>F</i> <sup>2</sup> ), <i>S</i>	0.083, 0.197, 1.17
No. of reflections	7889
No. of parameters	341
H-atom treatment	H-atom parameters constrained
	$w = 1/[\sigma^2(F_o^2) + (0.0325P)^2 + 151.7173P]$ where $P = (F_o^2 + 2F_c^2)/3$
Δρ <sub>max</sub> , Δρ <sub>min</sub> (e Å <sup>-3</sup> )	0.54, -0.58

**Table S2. Crystallographic data for 5**

	<b>5</b>
Crystal data	
Chemical formula	C <sub>42</sub> H <sub>102</sub> K <sub>2</sub> O <sub>12</sub> Si <sub>9</sub> ·C <sub>7</sub> H <sub>8</sub>
<i>M<sub>r</sub></i>	1222.37
Crystal system, space group	Triclinic, <i>P</i> -1
Temperature (K)	130
<i>a</i> , <i>b</i> , <i>c</i> (Å)	12.2789 (3), 16.4703 (3), 19.5884 (4)
α, β, γ (°)	74.5249 (19), 73.536 (2), 87.0261 (18)
<i>V</i> (Å <sup>3</sup> )	3660.14 (14)
<i>Z</i>	2
Radiation type	Mo <i>K</i> α
μ (mm <sup>-1</sup> )	0.32
Crystal size (mm)	0.59 × 0.31 × 0.20
Data collection	
Diffractometer	SuperNova, Dual, Cu at zero, Atlas
Absorption correction	Gaussian <i>CrysAlis PRO</i> 1.171.39.29c (Rigaku Oxford Diffraction, 2017) Numerical absorption correction based on gaussian integration over a multifaceted crystal model Empirical absorption correction using spherical harmonics, implemented in SCALE3 ABSPACK scaling algorithm.
<i>T</i> <sub>min</sub> , <i>T</i> <sub>max</sub>	0.415, 1.000
No. of measured, independent and observed [ <i>I</i> > 2σ( <i>I</i> )] reflections	73016, 16817, 13516
<i>R</i> <sub>int</sub>	0.035
(sin θ/λ) <sub>max</sub> (Å <sup>-1</sup> )	0.650
Refinement	
<i>R</i> [ <i>F</i> <sup>2</sup> > 2σ( <i>F</i> <sup>2</sup> )], <i>wR</i> ( <i>F</i> <sup>2</sup> ), <i>S</i>	0.046, 0.115, 1.06
No. of reflections	16817
No. of parameters	1089
No. of restraints	1928
H-atom treatment	H-atom parameters constrained
Δρ <sub>max</sub> , Δρ <sub>min</sub> (e Å <sup>-3</sup> )	0.60, -0.34

**Table S3. Crystallographic data for 6**

	<b>6</b>
Crystal data	
Chemical formula	C <sub>20</sub> H <sub>60</sub> Si <sub>10</sub>
<i>M<sub>r</sub></i>	581.58
Crystal system, space group	Triclinic, <i>P</i> -1
Temperature (K)	200
<i>a</i> , <i>b</i> , <i>c</i> (Å)	10.1167 (3), 12.4290 (3), 17.0543 (4)
α, β, γ (°)	71.232 (2), 80.544 (2), 69.194 (3)
<i>V</i> (Å <sup>3</sup> )	1894.96 (10)
<i>Z</i>	2
Radiation type	Mo <i>K</i> α
μ (mm <sup>-1</sup> )	0.36
Crystal size (mm)	0.41 × 0.26 × 0.08
Data collection	
Diffractometer	SuperNova, Dual, Cu at zero, Atlas
Absorption correction	Gaussian <i>CrysAlis PRO</i> 1.171.39.29c (Rigaku Oxford Diffraction, 2017) Numerical absorption correction based on gaussian integration over a multifaceted crystal model Empirical absorption correction using spherical harmonics, implemented in SCALE3 ABSPACK scaling algorithm.
<i>T<sub>min</sub></i> , <i>T<sub>max</sub></i>	0.370, 1.000
No. of measured, independent and observed [ <i>I</i> > 2σ( <i>I</i> )] reflections	36920, 8701, 7386
<i>R<sub>int</sub></i>	0.026
(sin θ/λ) <sub>max</sub> (Å <sup>-1</sup> )	0.650
Refinement	
<i>R</i> [ <i>F</i> <sup>2</sup> > 2σ( <i>F</i> <sup>2</sup> )], <i>wR</i> ( <i>F</i> <sup>2</sup> ), <i>S</i>	0.029, 0.077, 1.06
No. of reflections	8701
No. of parameters	291
H-atom treatment	H-atom parameters constrained
Δρ <sub>max</sub> , Δρ <sub>min</sub> (e Å <sup>-3</sup> )	0.33, -0.27

**Table S4. Crystallographic data for 7**

	7
Crystal data	
Chemical formula	C <sub>97</sub> H <sub>204</sub> K <sub>4</sub> O <sub>24</sub> Si <sub>16</sub>
<i>M</i> <sub>r</sub>	2360.43
Crystal system, space group	Monoclinic, <i>P2<sub>1</sub>/n</i>
Temperature (K)	110
<i>a</i> , <i>b</i> , <i>c</i> (Å)	13.3319 (3), 21.5603 (5), 23.7767 (6)
β (°)	99.786 (2)
<i>V</i> (Å <sup>3</sup> )	6734.9 (3)
<i>Z</i>	2
Radiation type	Mo <i>K</i> α
μ (mm <sup>-1</sup> )	0.33
Crystal size (mm)	0.46 × 0.20 × 0.09
Data collection	
Diffractometer	SuperNova, Dual, Cu at zero, Atlas
Absorption correction	Gaussian <i>CrysAlis PRO</i> 1.171.39.29c (Rigaku Oxford Diffraction, 2017) Numerical absorption correction based on gaussian integration over a multifaceted crystal model Empirical absorption correction using spherical harmonics, implemented in SCALE3 ABSPACK scaling algorithm.
<i>T</i> <sub>min</sub> , <i>T</i> <sub>max</sub>	0.425, 1.000
No. of measured, independent and observed [ <i>I</i> > 2σ( <i>I</i> )] reflections	101881, 15458, 12767
<i>R</i> <sub>int</sub>	0.043
(sin θ/λ) <sub>max</sub> (Å <sup>-1</sup> )	0.650
Refinement	
<i>R</i> [ <i>F</i> <sup>2</sup> > 2σ( <i>F</i> <sup>2</sup> )], <i>wR</i> ( <i>F</i> <sup>2</sup> ), <i>S</i>	0.050, 0.110, 1.07
No. of reflections	15458
No. of parameters	1366
No. of restraints	3528
H-atom treatment	H-atom parameters constrained
Δρ <sub>max</sub> , Δρ <sub>min</sub> (e Å <sup>-3</sup> )	1.00, -0.72



Computer programs: *CrysAlis PRO* 1.171.39.29c (Rigaku OD, 2017), *SHELXS2018/3* (Sheldrick, 2018), *SHELXL2018/3* (Sheldrick, 2018), *SHELXTL* v6.10 (Sheldrick, 2008).

#### 4. References

- 1 R. Fischer, T. Konopa, S. Ullly, J. Baumgartner and C. Marschner, *J. Organomet. Chem.*, 2003, **685**, 79–92.
- 2 G. Sheldrick, *Acta. Cryst.*, 2015, **C71**, 3-8.